



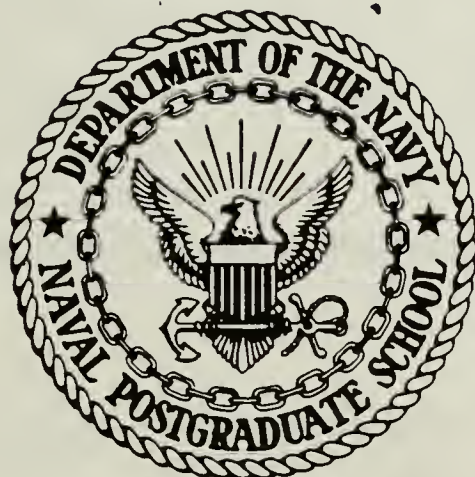
DUDLEY KNOX LIBRARY  
NAVAL POSTGRADUATE SCHOOL  
MONTEREY, CALIFORNIA 93943





# NAVAL POSTGRADUATE SCHOOL

## Monterey, California



# THESIS

THE INFLUENCE OF LARGE-SCALE 200 MB  
TROPICAL DIVERGENCE EVENTS ON THE  
MIDLATITUDE ZONAL FLOW OVER THE  
ASIA-PACIFIC REGION DURING THE  
1983-84 WINTER

by

Keng-Gaik Lum

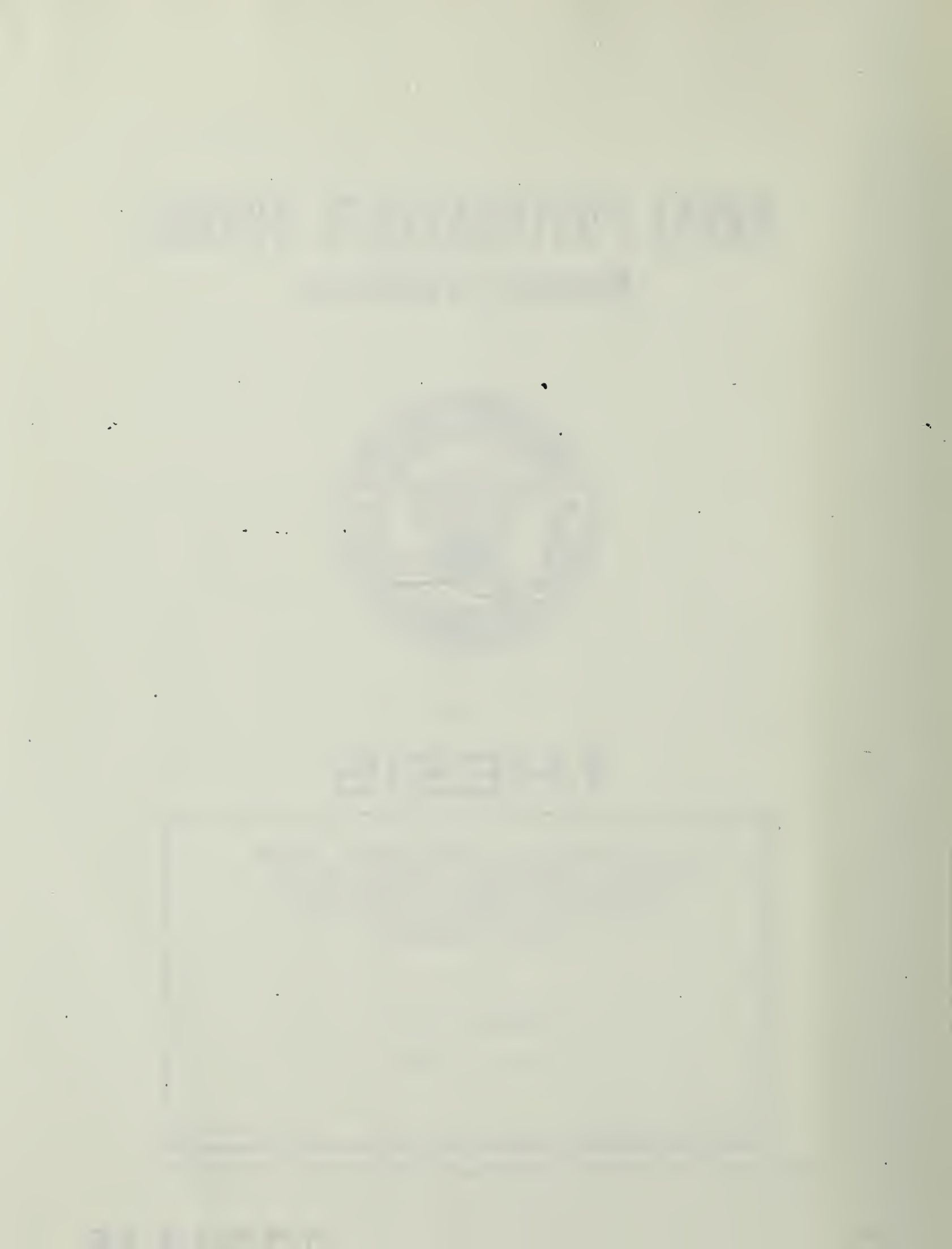
June 1985

Thesis Advisor

C.-P. Chang

Approved for public release; distribution unlimited.

T222878



UNCLASSIFIED

SECURITY CLASSIFICATION OF THIS PAGE (When Data Entered)

midlatitudes. Three cases of the tropical divergence events were associated with tropical storm activities. This association asserts that westerly jet intensification is, in fact, a response to the tropical divergence enhancement, accepting the view that developed tropical storms are tropically-forced systems. A case of tropical divergence enhancement was also found to be attributable to a cold surge, reaffirming the importance of the cold surge related jet acceleration. Further, the study also confirms the downstream propagation of the jet streak; the existence of thermally indirect circulations at the jet exit region of the jet, both in the time-mean and in the transient motion fields.

UNCLASSIFIED

Approved for public release; distribution unlimited

The Influence of Large-Scale 200 mb Tropical  
Divergence Events on the Midlatitude Zonal Flow  
over the Asia-Pacific Region During the 1983-84 Winter

by

Keng-Gaik Lum  
Malaysian Meteorological Service  
B.S. (Hons), University of Malaya, 1976

Submitted in partial fulfillment of the  
requirements for the degree of

MASTER OF SCIENCE IN METEOROLOGY

from the

NAVAL POSTGRADUATE SCHOOL  
June 1985

## ABSTRACT

Global band analysis grid point data produced by FNOC for the 1983/1984 winter season are used to study the daily variation of the midlatitude 200 mb zonal wind in relation to the divergence field. It is found that the enhancements of tropical divergence are well correlated with the intensification of the westerly jet in the midlatitudes. Three cases of the tropical divergence events were associated with tropical storm activities. This association asserts that westerly-jet intensification is, in fact, a response to the tropical divergence enhancement, accepting the view that developed tropical storms are tropically-forced systems. A case of tropical divergence enhancement was also found to be attributable to a cold surge, reaffirming the importance of the cold surge related jet acceleration. Further, the study also confirms the downstream propagation of the jet streak; the existence of thermally indirect circulations at the jet exit region of the jet, both in the time-mean and in the transient motion fields.

## TABLE OF CONTENTS

I.	INTRODUCTION -----	9
II.	DATA AND METHOD OF COMPUTATION -----	15
III.	TIME-MEAN FIELDS -----	19
IV.	DAY-TO-DAY VARIATIONS -----	21
	A. LONGITUDINAL-TIME SECTIONS OF MIDLATITUDE ZONAL WIND AND EQUATORIAL VELOCITY POTENTIAL . -----	21
	B. EXAMINATION OF SELECTED REGIONS FOR DECEMBER -----	25
V.	CORRELATION BETWEEN VELOCITY POTENTIAL AND ZONAL ACCELERATION -----	33
VI.	SUMMARY OF RESULTS AND CONCLUSIONS -----	37
	LIST OF REFERENCES -----	64
	INITIAL DISTRIBUTION LIST -----	66

## LIST OF FIGURES

1. The December 1983 mean 200-mb horizontal wind vectors with isotachs (labels in m/s) a; and velocity potential (isopleth interval =  $2.5 \times 10^6 \text{m}^2/\text{s}$ ), b. ----- 40
2. As Fig. 1 except for January 1984. ----- 41
3. As Fig. 1 except for February 1984. ----- 42
4. As Fig. 1 except for the winter season 1983/84. ----- 43
5. The 200-mb horizontal wind vectors with isotachs (labels in m/s) for 25 Dec 1983 (00Z), a; and velocity potential (isopleth interval  $2.5 \times 10^6 \text{m}^2/\text{s}$ ) for 25 Dec 1983 (00Z), b. ---- 44
- 6a. Longitude-time section of midlatitude zonal velocity (interval 10 m/s) averaged over 25N-40N for December. The axes of maxima and minima are denoted by dark solid and dashed lines, respectively. Letters A, B, C, D, D' and E identify significant events of jet strengthening ----- 45
- 6b. Longitude-time section of tropical velocity potential (interval  $2.5 \times 10^6 \text{m}^2/\text{s}$ ) averaged over 0-18N of December with areas  $> 7.5 \times 10^6 \text{m}^2/\text{s}$  hatched and that  $> 12.5 \times 10^6 \text{m}^2/\text{s}$  dotted. Dark solid and dashed lines indicating jet maxima and minima, respectively are copied from Fig. 6a. ----- 46
- 7a. Longitude-time section of midlatitude zonal velocity (interval 10 m/s) averaged over 25N-40N for January. The axes of maxima and minima are denoted by dark and dashed lines, respectively. ----- 47
- 7b. Longitude-time section of tropical velocity potential (interval =  $2.5 \times 10^6 \text{m}^2/\text{s}$ ) averaged over 0-18N of January with areas  $> 7.5 \times 10^6 \text{m}^2/\text{s}$  hatched and that  $> 12.5 \times 10^6 \text{m}^2/\text{s}$  dotted. Dark solid and dashed lines indicating jet maxima and minima, respectively are copied from Fig. 7a. ----- 48
- 8a. As Fig. 7a except for February. ----- 49
- 8b. As Fig. 7b except for February. ----- 50
9. Locations of areas for averaging zonal velocity in the midlatitudes and the tropical divergence. ----- 51
10. As Fig. 1 except for the period 17-26 December 1983. ----- 52

11a.	Time series of area-averaged zonal velocity for the Tibetan Plateau region (TP), (80-110E, 25-40N). -----	53
11b.	Time series of area-averaged horizontal divergence for the equatorial Indian Ocean region (IO), (70-90E, 5S-10N). -----	53
12.	Time series of minimum reported pressure in the Indian Ocean region (IO), (60-90E, 20S-10N). -----	54
13a.	As in Fig. 11a except for the East Asia-western North Pacific Ocean region (EA), (110-140E, 25-40N). -----	55
13b.	As in Fig. 11b except for the maritime continent region (MC), (90-115E, 5S-10N). -----	55
14.	Storm tracks for (a) Sperry and (b) Thelma. -----	56
15.	As Fig. 1 except for the period 14-18 December 1984. -----	57
16.	As Fig. 1 except for the period 1-5 December 1984. -----	58
17	Vector sum of 200-mb divergent velocity over the region (125-135E, 20-25N) showing the strengthening of the return flow. -----	59
18a.	As in Fig. 11a except for the region east of Japan (EJ), (130-160E, 25-40N). -----	60
18b.	As in Fig. 11b except for the region east of the Philippines (EP), (130-145E, 10-20N). -----	60
19a.	As Fig. 11a except for the northern central North Pacific Ocean region (NP), (160-140W, 25-40N). -----	61
19b.	As Fig. 11b except for the tropical central North Pacific Ocean region (CP), (180-150W, 5-25N). -----	61
20.	Correlation coefficients between tropical velocity potential and zonal acceleration in the midlatitudes (a) December 1983, (b) January 1984 and (c) February 1984. -----	62
21.	Time-lag correlation coefficients between tropical velocity potential and zonal acceleration in the midlatitudes for (a) northern hemisphere (winter) 1983/84 and (b) southern hemisphere (summer) 1983/1984. -----	63

#### ACKNOWLEDGEMENT

I would like first and foremost to thank Professor C.-P. Chang for his tireless guidance and continual encouragement throughout the whole development and writing of this thesis. My thanks also go to Professor James Boyle who had generously assisted me in using many of his computer programs and had offered many valuable pointers in the data analysis. I am grateful also to Dr. Hock Lim, who (fortunate for me) was visiting the Naval Postgraduate School, for his valuable suggestions and enlightening explanations to concepts related to this work. In addition, Professor Robert Renard for his thorough reading of the manuscript and many suggestions for improvement. Finally, I wish to thank the National Oceanic and Atmospheric Administration, Office of International Training, for sponsoring my education at NPS, and the World Meteorological Organization Fellowship Program for providing the financial support.

## I. INTRODUCTION

Tropospheric westerly jet stream systems have traditionally been classified according to the atmospheric general circulation (Palmen and Newton, 1969) into two categories, viz., the polar front and subtropical jet streams. The former is well-recognized to be associated with the deep low-level frontal zones of the extratropics and possesses great temporal as well as spatial variability. The subtropical jet stream system on the other hand is characterized by greater steadiness both in the direction and geographical location. It is also very much confined to the upper troposphere.

The term general circulation as it was used in the 1960's generally referred to zonal symmetric circulation, i.e., the meridional profile obtained by taking zonal averages of the physical and dynamical quantities such as zonal velocity, meridional velocity and diabatic heating. The treatise work of Lorenz (1967) for example is largely devoted to the dynamics and the history of the development of such circulations. In this context, the Hadley cell may be viewed as a statistical averaged phenomenon in the tropics and the subtropics that arises by virtue of the zonally-averaged meridional temperature gradient. From this viewpoint, nothing could be said about the differences between one longitude and another longitude sector.

The position of the subtropical westerly system with respect to the Hadley cell led to the inference that this wind system arose because of the partial conservation of angular momentum on the poleward-moving air

parcels. To substantiate this concept, Palmen and Newton (1969; section 1.4) proceeded to estimate the time required for an air parcel to move from the equatorial belt to the subtropics using the meridional velocity of the zonally-symmetric Hadley cell. The value obtained is on the order of a week.

The winter subtropical jet system has been shown by Krishnamurti (1961) and others to manifest a three-wave pattern around the globe. It is obviously not possible to explain the longitudinal variations in the wind speed in terms of the zonally-symmetric circulation. While completely satisfactory mechanism(s) to explain the locality of the three winter mean jet maxima is(are) still lacking, it is also worthwhile to find answers to their variations in location and strength on a much shorter time scale. They are quite obviously related problems; the knowledge of one may well assist to unlock the other.

Keen interest is seen in the last decade or so on the zonal asymmetric nature of the large-scale circulation (Blackmon et al., 1977; Hoskin and Pearce, 1983). Part of the reason may be due to the availability of the grid-point data from routine global NWP products. Also, perhaps more importantly is the general belief that the asymmetric aspect of large-scale circulation contains insights crucial to the understanding of many phenomena such as monsoon cold surges, life-cycle of extratropical storm and the related maintenance of the jet stream.

In many previous studies, time-mean structures of the motion field were studied. Krishnamurti et al. (1973), for example, emphasized the

presence of a strong three-wave pattern in the 200 mb velocity potential and streamfunction and the presence of an east-west circulation in addition to the East Asia local Hadley cell. A large mass source was found over the equatorial southeast Asia in the northern winter which formed the rising branch of the local Hadley and east-west circulations. On the other hand, in a study related to the midlatitude zonal asymmetry, Blackmon et al. (1977), using nine-year winter data found that there was no convergence of eddy flux of westerly momentum in the region upstream of the time-mean jet stream (250 mb). Since a rapid increase of westerly flow in the zonal direction occurred in this region, a time-mean meridional, thermally direct circulation was necessary to account for the spatial acceleration. Likewise, time-mean equatorward flow at the jet level of a thermally indirectly circulation was necessary to explain the spatial deceleration at the jet exit and to counteract the strong convergence of westerly momentum flux observed to the north of the jet exit. Low tropospheric heat fluxes and wind consistent (in terms of quasi-geostrophic theory) with the existence of the two time-mean meridional circulations were also observed. Evidence is accumulating for the existence of the thermally direct circulation at the westerly jet entrance region and the existence of a thermally direct circulation at the jet exit region.

Meanwhile, in a different line of investigation, Ramage (1971) and Chang et al. (1979) attributed the intensification of the East Asia local Hadley cell and the enhancement of the tropical convection over

the maritime continent to the occurrences of cold surges over East Asia. A similar phenomenon has also been observed by Bosart (1973) in the Caribbean Sea region. Further investigations on the cold surges by Chang and Lau (1982) and Lau et al. (1983), using a composite technique, established a sequence of events which they termed a 'short-term teleconnection', relating the vacillations of the East Asia jet to the waxes and wanes of the East Asia local Hadley cell and the Walker circulation. An important difference between the study of Blackmon et al. (1977) and the works of Chang et al. (1979), Chang and Lau (1982) and Lau et al. (1983) is that the latter examined the cold surge phenomenon and jet stream in a much smaller time scale (on the order of a few days), as compared with the former which made deductions from time-mean (over nine winters) structures of geopotential height, heat and momentum fluxes. However, results obtained from composite studies could represent only an averaged behaviour. To what extent that individual cases may vary from the sequence is a question that can be answered only when the full dynamics of the 'teleconnection' is known. A point that is certain is that the term 'teleconnection' as applied in this context has already been evolved and become quite divorced from that originally used by Bjerknes (1969) because of the short time scale involved. Energy and momentum transports by physical movement of air parcels as discussed earlier require time on the order of a week for the midlatitudes to feel the intensification of Hadley cell originating from the tropics, in contradiction to the transient interaction apparently

observed. Theoretical investigations by Lim and Chang (1983) provided further clues to the mechanisms of the short-term teleconnection. Gravity-wave type motion appears to be the 'agent' for the momentum and energy transports.

Since cold surge occurrences are associated with enhanced mid-latitude baroclinicity (Chang and Lau, 1982; Lau et al., 1983; Boyle, 1983), the strengthening of the jet possibly could be a solely midlatitude event, quite independent of the tropical convection. Thus, one question that needs to be answered is how and what effect has the tropical convection, as a manifestation of the rising branch of the local Hadley cell, affect the midlatitude westerly jet stream. This problem may be viewed as a feedback of the tropics to the midlatitudes following monsoon cold surges as it is suggested by Chang and Lau (1982) and Lau et al. (1983); or alternatively it may be viewed as a separate tropical forcing on the midlatitudes. In this study, correlation between the midlatitude zonal wind and the tropical divergence variation in the winter 1983/84 is examined; individual cases of correlative variations in December 1983 are identified.

In the context of short-term teleconnection and monsoon cold surges, the term subtropical jet stream over Asia is not quite applicable because cold surges are often associated with strong low-level baroclinic zones pushing much further south than the winter seasonal mean subtropical jet latitudes. The distinction between the subtropical and polar-front jet systems on a day-to-day basis becomes obscure.

Thus, in this work, the jets are identified by their geographical locations. In the same vein, since midlatitude westerlies expand much farther south during winter, the term 'midlatitudes' will in general be used to include part of the subtropics, as equatorward as 25N.

## II. DATA AND METHOD OF COMPUTATION

The global band analyses (GBA), produced by the Fleet Numerical Oceanography Center (FNOC) at 12-hour intervals, are provided on a 49 x 144 Mercator projection (true at 22.5N) grid. The domain of analysis is the band from 40S to 60N about the globe.

The 1983/1984 winter data are used in this study. For the three months concerned (Dec 83 through Feb 84), there are nominally 182 twice daily observation times. No data are available for 16 observation times. Therefore, these are interpolated linearly in time whenever continuous data are required. Although the FNOC analysis uses a variational approach to integrate temperature and winds in the vertical, 200 mb is the top boundary of the analysis and is analyzed strictly with a two-dimensional successive correction method without the influence of temperature or wind field from other levels. The analysis incorporates all available real time data using 6-h persistence as the first guess and is not used as an input to any numerical weather prediction model. In regions of adequate data coverage, the analyzed data may be more suitable than other operationally produced analyses, especially for the purpose of studying tropical divergence. This is because presently it is the only operational analysis that does not make use of model-forecast tropical divergence as the first guess. The representativeness of the model-dependent divergence is still a subject for debate (Julian,

1984). Furthermore, the FNOC analysis is also free from the bias of midlatitude-determined structure functions used in optimal interpolation scheme which tends to suppress synoptic scale divergence in the tropics. Owing to the availability of geostationary satellite-derived winds and aircraft data, the 200 mb data coverage over the tropical Pacific and Indian Oceans was relatively adequate during the period of study.

The 200 mb zonal ( $U$ ) and meridional ( $V$ ) velocities are used to compute the relative vorticity ( $\zeta$ ) and divergence ( $\delta$ ) from which the streamfunction ( $\psi$ ) and velocity potential ( $X$ ) are computed. Because of the presence of the horizontal boundaries at 60N and 40S, a boundary condition is required to solve for velocity potential by the method of relaxation, as in the approach used by Hawkins and Rosenthal (1965), in which the velocity potential is set to zero at both boundaries. The equations used are as follows:

$$\nabla^2 \psi = \zeta = \left( \frac{\partial V}{\partial X} - \frac{\partial (U \cos \psi)}{\partial Y} \right) \sec \phi \quad (1)$$

$$\nabla^2 X = -\delta = -\left( \frac{\partial U}{\partial X} + \frac{\partial (V \cos \psi)}{\partial Y} \right) \sec \phi, \quad (2)$$

where  $x$  and  $y$  are the horizontal coordinates in the Mercator projection. They may be calculated by

$$x = a \lambda \quad (3)$$

$$y = a \ln\left(\frac{1 + \sin\phi}{\cos\phi}\right) \quad (4)$$

For projection true at 22.5 degrees,  $a = R \cos(22.5)$ , where  $R$  is the radius of the earth. The  $\lambda$  and  $\phi$  are the longitude and the latitude in the spherical coordinate system.

The north-south boundary condition used is that the velocity potential equals to zero at all times. This use of the boundary condition also produces some unavoidable deleterious effect near the boundaries. However, comparison with the National Meteorological Center's (NMC) monthly mean analyses, which are fully global (with no horizontal boundaries), shows that the main features 10 degrees latitude or so away from the boundaries appear unaffected. A very detailed comparison is, of course, not possible because the divergence field of the NMC analyses in the tropic is strongly model-dependent.

Because of the inclusion of a minus sign on the right of the equation (2), velocity potential maximum (positive) has a general association with divergence rather than convergence. It must be noted that the extremum of velocity potential is only coincidental with the divergence extremum if they are sinusoidal functions as the latter is the second derivative of the first. In the real atmosphere the coincidence is not guaranteed, in general.

For the determination of the dates of cold surges, surface data from GBA are also used. The FNOC daily surface analyses were also available for reference..

### III. TIME-MEAN FIELDS

The monthly mean 200 mb horizontal wind vector and velocity potential fields for the months December 1983, and January and February 1984, are depicted in Figs. 1, 2 and 3. Also shown (Fig. 4) are the winter seasonal mean vector wind and velocity potential.

Of special interest to this study is the longitudinal locations of the jets. Using the 40 m/s isotach to delineate the jet streak, it is seen that the American jet is smaller than the East Asian jet in longitudinal extent. Also, the latitudinal position of the American jet shown in December, January and February monthly means varies from about 40N to 45N and then to about 25N. In January, the jet streak is more extensive and is tilted NE-SW. By comparison, the East Asian jet exhibits considerably less latitudinal variability.

The seasonal-mean velocity potential fields (Fig. 4b) indicates the presence of a vast area of tropical divergent flow, centered over the east-west oriented maritime continent and extending longitudinally in both directions. To the east-southeast, the central axis extends deeply into the tropical southeastern Pacific, representing the outflow of the South Pacific Convergence Zone (SPCZ). To the west and the southwest, it extends to the tropical South Africa covering the equatorial Indian Ocean. Individual months (Figs. 1b, 2b and 3b) also exhibit essentially similar features, though in January the primary dominant divergence appears to have shifted to the equatorial Indian Ocean from maritime

continent. Apart from this, the structure of the Indian-and-Pacific Ocean divergence area is close to normal as may be seen by comparison with the 10-year (1973/74-1982/83) winter seasonal and monthly means produced by Boyle and Chang (1984). Another equatorial divergence area is also found over the South American continent which extends to the eastern South Pacific Ocean.

Another feature in the velocity potential distribution worth noting is the relative minimum center found between 10N-20N in the central North Pacific Ocean. This minimum together with the relative maximum north of it reflects the presence of a reversed Hadley circulation. This is in accord with Blackmon et al.'s (1977) deduction of the existence of the thermally indirect circulation at the time-mean jet exit area, based on quasi-geostrophic theory. The juxtaposition of the SPCZ south of this relative minimum also implies a local meridional circulation, with rising air from the SPCZ.

#### IV. DAY-TO-DAY VARIATIONS

##### A. LONGITUDINAL-TIME SECTIONS OF THE MIDLATITUDE ZONAL WIND AND EQUATORIAL VELOCITY POTENTIAL

Daily velocity potential and wind vector plots show that although the essential large-scale features remain unchanged the relative strength of the jet maxima varies considerably. These plots suggest a relationship between the occasional sudden increases in the tropical velocity potential and locality of the jet maxima. As an example, the 25th of December (Fig. 5b) sees a shift of the major velocity potential maximum from the climatological position of the maritime continent to the Indian Ocean. The usually much weaker jet over the Arabian Peninsula on this day shows comparable strength to the East Asian jet (Fig. 5a).

In order to make systematic comparisons between the longitudinal positions of the velocity potential extrema and the zonal wind intensification, longitudinal-time sections of the zonal wind ( $U$ ) and the velocity potential ( $\chi$ ) are plotted. Because of the daily mobility of the velocity potential maxima over a broad latitudinal band, averaged velocity potential from the equator to 18N is presented. Figs. 6b, 7b and 8b depict the time sections for December 1983, January 1984 and February 1984, respectively. Similarly, the zonal wind values are averaged from 25N and 40N. The sections are shown along with that of velocity potential as Figs. 6a, 7a and 8a. In order to restrict the

scope of the study, the longitudes in these sections are confined only to 40E and 100W.

For the longitude-time sections of zonal wind, the contour interval used is 10 m/s. Because of the sign convention adopted in the computation of velocity potential, a maximum, given due consideration to the discussion in section II, has a general association with divergence. In the velocity potential sections, negative, zero and positive contours are drawn dotted, heavy and solid, respectively. The relative maximum areas of velocity potential value above  $7.5 \times 10^6 \text{m}^2/\text{s}$  are hatched and that above  $1.25 \times 10^6 \text{m}^2/\text{s}$  are dotted. The isopleth interval used is  $2.5 \times 10^6 \text{m}^2/\text{s}$ .

### 1. December

In the longitude range 40E to 100W depicted, five main zonal velocity maxima are noted. They are located within 80E and the date line (180E). Generally speaking, weak westerlies are found in the longitudinal band between 170W and 130W. An eastward propagation pattern in many parts of the figure is apparent with an average speed of approximately 10 degrees of longitude per day. In particular, the maximum located at about 100E on the 21st appears to have moved a longitudinal distance of 50 degrees in four days. This eastward propagation is similar to that following intensification of the East Asia local Hadley cell after a cold surge event observed by Chang and Lau (1982) and Lau et al. (1983). Their analysis of the momentum

equation suggests that the propagation is primarily due to the advection of zonal momentum by zonal velocity ( $udu/dx$ ).

Using the shape of the 60 m/s and 70 m/s mean isotachs as guide, heavy solid lines are marked on Fig. 6a to identify the five episodes of westerly zonal wind intensifications. The five episodes are labeled by the letters A (2-5 December), B (8-11 December), C (13-20 December), D (20-25 December), and E (26 December - beginning of January), respectively. Episode D also branches into two axes, one remaining stationary between 90-95E and the other, labeled D', propagating eastward to about 150E. These episodes will be referred to in the following discussion. Thus, the rapid decelerating regions lie, in general, between the solid and dashed lines; immediately upstream of the solid lines usually lie the accelerating areas. For ease of comparison, these lines are also transferred to the velocity potential longitude-time section (Fig. 6b). Note that unlike the zonal wind maxima the velocity potential maxima do not show any tendency of longitudinal movement to the east. The relative minima downstream of the jet maxima are also marked, in these cases with heavy dashed lines. From this figure, it becomes clear that the major velocity potential maxima have the tendency to locate slightly upstream (west) of the zonal velocity maxima; and on approximately the same days. Likewise, major minimum velocity potential centers found between 180E and 120W also correspond in longitudes and time with the zonal westerly wind minima, with the

latter displaced somewhat downstream. This implies a frequent co-locations (with respect to longitude as well as time) of zonal accelerations (decelerations) with the equatorial velocity potential maxima (minima), strongly suggesting a cause-effect relationship.

## 2. January and February

The relationship suggested by the longitude-time sections of December appears to hold for January and February as well. In Fig. 7a, four episodes (F, G, H, I/I') of intensifications of the zonal wind are indicated in January and they have clear velocity potential maxima (hatched and dotted) over the jet streak entrance longitudes. There is also an event of jet intensification whose jet entrance is at about 140E occurs on day 7.5. An extension of episode E discussed for December can also be identified on the first three days of the month. The propagation of jet streak discussed earlier is even more pronounced for this month.

Except for H, the jet exit regions, which lie between the solid lines and the dashed lines downstream, also coincide with the velocity potential minima.

The February zonal velocity longitude-time section (Fig. 8a) shows generally a large area of above-60 m/s zonal velocity covering from 100E to 170E almost for the whole month making identification of organized strengthening-weakening of zonal wind difficult. Eastward propagation that is so clearly indicated for December and January is not

at all obvious for this month. Clear-cut instances of velocity potential enhancements are also lacking over the 100E to 170E longitudinal sector as may be seen from Fig. 8b. In the entire eastern hemisphere ten small regions of velocity potential  $> 7.5 \times 10^6 \text{ m}^2/\text{s}$  are found in this 29-day longitude-time section. However all of these are of duration less than two days and, with the exception of the one occurrence on 28 February, none of the velocity maxima reach  $10 \times 10^6 \text{ m}^2/\text{s}$  (one isopleth within the hatched area). Thus, events of significant tropical divergence observed in the previous months are not found in February. The absence of a significant tropical divergence event and the lack of zonal wind strengthening-weakening for this month may be viewed as a negative evidence of the effect of tropical divergence on the midlatitude jet. Over the longitude sector east of the date line, comparison of Fig. 8a and 8b shows that the decelerating regions over the jet exits coincide with the velocity potential minima very well, reflecting the close relationship between the mid-Pacific trough and the jet exit indirect circulation.

#### B. EXAMINATION OF SELECTED REGIONS FOR DECEMBER

In this section, the different episodes of apparent transient tropical-midlatitude interactions are examined in greater detail. In order to highlight these events, time series of areal averages of divergence and zonal wind are plotted. Fig. 9 gives the geographical locations of the chosen areas along with the symbols used to designate

the areas. As before, boxes for averaging zonal wind are delimited by the parallels 25N and 40N. In view of the discussion in Section IV.A, longitudes are chosen to be somewhat downstream (east) of the tropical divergence areas. The transient interactions may then be studied by taking the divergence and zonal wind in pairs.

1. Divergence over IO (70-90E, 5S-10N) and Zonal Velocity over TP (80-110E, 25-40N)

Since D is the only event which indicates enhanced upper-level divergence over the Indian Ocean, the global band 200 mb wind and velocity potential for the period 17-26 December are first averaged and shown in Fig. 10. Compared to monthly means (Fig. 1), it is clear that the East Asian jet core (as defined by the 60 m/s isotach) is stretched westward by about 25 degrees in longitude to cover the Tibetan Plateau. This corresponds to a westward shift of the tropical velocity potential center from its December mean position to the central and eastern equatorial Indian Ocean. As a consequence of the latter the northeastward divergent circulation, as suggested by the velocity potential gradient, may be viewed as the main East Asian Hadley cell during this 10-day period.

Fig. 11 compares the time series of the western side of the jet core, as represented by the zonal velocity averaged over TP, the Tibetan Plateau (80-110E, 25-40N), and that of the equatorial Indian Ocean divergence averaged over IO (70-90E, 5S-10N). The zonal velocity shows a major peak from 16-27 December, corresponding to episode D in

Fig. 6. An overall agreement can be readily seen in the divergence series, whose value is significantly higher than zero only during this period. To further ascertain the association of this flare-up in divergence with tropical convection, the surface weather maps during the same period produced by NMC and FNOC are examined; they which show an active equatorial trough in the equatorial Indian Ocean box with a developed tropical depression between 20-24 December. Fig. 12 is a plot of the minimum sea-level pressure observed in the IO box, which reflects the presence of this storm (the dip on 12 GMT, 7 December is due to the activity of a tropical storm in the southwestern Indian Ocean which moved briefly to the western edge of the averaging box). Inspection of the satellite imagery further confirmed that the enhanced divergence associated with episode D is indeed due to the convection of the active equatorial trough and the tropical storm.

In addition to the acceleration of the zonal wind over the Tibetan Plateau, during episode D the strengthening of the midlatitude jet also propagated eastward for several days into the region of the monthly mean jet core corresponding to the episode D'.

2. The Divergence of MC (90-115E, 5S-10N) and Zonal Velocity over EA (110-140E, 25-40N)

Fig. 13 shows the comparison between the zonal wind averaged over East Asia EA (110-114E, 25-40N) and the divergence averaged over MC (90-115E, 5S-10N). As may be seen from Fig. 1, the former area covers the western half of the December mean East Asia jet core, and the latter area covers the December mean velocity potential center over the maritime continent. Both time series show three major oscillations with nearly identical peaking dates viz, December 3, 14 and 24. There were no developed organized convective events such as tropical cyclones reported in the maritime continent during this period. Papers reviewed in the introduction show that enhanced convection over this region in many cases may be forced by monsoon cold surges. Usually the convection is sustained for several days after the onset of cold surges. For the purpose of determining the occurrences of cold surges, the time series of the area average (110-120E, 17-20N) of the northerly surface winds computed from the GBA grid point data has been used. The definition of cold surges as it was used by Chang and Lau (1982) comprises two parts: (1) an increase of 5 m/s or more in the area-averaged northerly surface wind over 12-24 hours; (2) the increased wind must sustain above 7 m/s for three days or more. With the above criteria, four surges may be identified during this winter. The first occurrence from 12 GMT 20 December until 12 GMT 9 January appears to consist of a multiple of cold surges, the first of which began on the 20th December and then the

surface wind relaxed slightly before the second push on 26 December. The increase in divergence shown in Fig. 11b, starting 20 December, may be attributed to the forcing of the cold surge. During the first surge impulse, the maximum divergence center was shifted to the eastern Indian Ocean (episode D) due to tropical storm activity there. The second surge impulse can be clearly identified as episode E in Fig. 6. The increase in the zonal velocity during the last ten days of December shown in Fig. 11a agrees well with the two-impulse cold surge. The first part of this period (21-25 December) is also influenced by the downstream propagation of the jet maximum (episode D' in Fig. 6a).

### 3. The Divergence over EP (130-145E, 10-20N) and EJ (130-160E, 25-40N)

The box EP is not located over the December mean velocity potential maximum but rather over a weak velocity potential 'ridge' East of Philippines. Very large divergence fluctuations were observed over this area during the December month. Further, note that the area east of Japan, EJ, for averaging the zonal velocity lies over the eastern half of the December jet core.

Fig. 6 suggests that episodes of jet intensification identified as A and C are associated with major divergence enhancement events. These events coincide with the developed stage of two tropical storms, Sperry and Thelma. Both of these storms began as weak disturbances northwest of Papua New Guinea, strengthening as they tracked towards an area east of the Philippines. Fig. 14 shows the tracks when the storm

were relatively well-developed. In order to highlight the unclimatological shift of jet streak and the velocity potential maximum in concert with these events, the horizontal wind and velocity potential averaged over 14-18 December, the period when storm Thelma was active, are depicted in Fig. 15. Fig. 6b shows that this is also the maximum divergence period over the western Pacific for the entire month. Consistent with the storm activity, the major tropical velocity potential center is located to the east of Philippines just over the storm, considerably different from both Figs. 1b and 10b. The jet core also assumes a different pattern from that shown in Figs. 1a and 10a with a shorter longitudinal extent but stronger maximum velocity ( $> 80 \text{ m/s}$ ) centered at 150E. Furthermore, the anticyclonic circulation south of the jet core with a relatively short wave structure resembles the pattern of a Rossby mode response to a tropical heat source in the region of the observed tropical divergence center, as predicted by linear equatorial wave theories (e.g., Lim and Chang, 1983). This structure strongly indicates that storm Thelma had exerted a significant transient influence on the midlatitude motion. In fact, the amplified midlatitude wave pattern eastward of the East Asia jet may even suggest some downstream effect of the tropical heating predicted by the theories.

Fig. 16 shows the velocity potential and horizontal wind distribution averaged over the period (1-5 December) during which the

storm Sperry was well-developed. In this case, the relative maxima were found in the general tropical divergence area of the maritime continent, and the western and southwestern Pacific Ocean. Just as in the case of storm Thelma, the strongest divergent velocity emanating from this large tropical divergence area was found between an area east of the Philippines where the storm was located, and the East China Sea. This can be seen clearly from the velocity potential gradient ( $\nabla \chi$ ). As a separate depiction of the pronounced effect of the two tropical storms on the local Hadley circulation, the vector average of the divergent velocity  $\nabla \chi$  over the area between southeast China and the east of the Philippines (20-25N, 125-135E) is shown in Fig. 17. The sharp rise in ( $\nabla \chi$ ) to about 10 m/s in a steady southeasterly direction during the storm-active periods are clearly shown. Fig. 18 shows the time series of the averaged divergence over EP and the averaged zonal velocity over the area just east of Japan (EJ). The first two peaks reflect clearly the effect of the storms. The last major peak in the zonal velocity series was not due to the tropical forcing but to the advection from upstream. This is consistent with the fact the episode E has an extended downstream propagation (Fig. 6).

#### 4. Convergence over CP (180-150W, 5-25N) and Zonal Velocity over NP (160-140W, 25-40N)

Fig. 19 shows a different feature from what has been emphasized thus far. The mean December and winter divergence distributions (Figs. 1b and 4b) show that the area chosen was convergence area lying in the

mean mid-Pacific trough (Figs. 1a and 4a). Three periods of reduced zonal velocity in the North Pacific jet exit region (NP) may be noted viz., 3-6 December, 13-24 December and 27-31 December from Fig. 19. Despite the rather noisy convergence series of the tropical Central Pacific (CP), the relation between the reduction of zonal velocity in NP and the increase in convergence in CP is strikingly clear. This transient interaction between the jet and the convergence area south of it is consistent with the conclusion drawn by Blackmon *et al.* (1977), that the time-mean jet requires an indirect circulation at the jet exit region. Referring back to the zonal velocity and the velocity potential longitude-time sections in Fig. 6, where heavy dashed lines are used to indicate the zonal velocity minima, these three periods of reduced zonal velocity and increased convergence appeared to be subsequential to the episodes of upstream jet intensification; the first period (3-6 December) may be related to episode A, the second period (13-24 December) may be related to B, and the last period (27-31 December) related to D' and E. A plausible sequence of events beginning from an increase of tropical convection, then followed by jet intensification, downstream jet deceleration at the jet exit region and convergence enhancement south of the jet exit area is suggested by these results. However, more extensive studies are needed to confirm this hypothesis.

## V. CORRELATION BETWEEN VELOCITY POTENTIAL AND ZONAL ACCELERATION

The results presented earlier give convincing evidence that over several regions in the Asia and Pacific Ocean region, the variation of the tropical divergence corresponds very well with that midlatitude zonal wind, in spite of the fact that local changes of zonal wind also may be due to advection from upstream and other mechanisms. In order to have a better view of the geographical preference of such transient tropical-midlatitude interactions during winter, linear correlation coefficients are calculated for the tropical velocity potential averaged between the equator and 18N for all longitudes and the averaged zonal wind between 25N and 40N. Acceleration is used here because of the apparent simultaneous occurrences of the acceleration and velocity potential over the same longitudes as seen in the longitude-time sections presented above. The acceleration is approximated by

$$\frac{du}{dt} = \frac{\partial u}{\partial t} + u \frac{\partial u}{\partial x} \quad (5)$$

$$= fv_x, \quad (6)$$

assuming negligible meridional and vertical advections. The second equality comes about because the Coriolis torque on the meridional geostrophic (assumed mostly rotational) wind is cancelled by the zonal

pressure gradient, leaving behind only the torque on the meridional divergent part available to give rise to zonal acceleration. Thus, this equation shows that the Coriolis torque on the 200 mb return flow of the local Hadley circulation plays a role in the change of the midlatitude jet. Fig. 20 graphs the correlation coefficients against the longitudes. Also included are the 2.5% and the 5% significance levels, computed using the analysis of variance. Panofsky and Brier (Ch. IV, 1968) discuss the problems in applying this approach in meteorological series, one of which pertains to the presence of autocorrelation. To somewhat redress this problem, the degrees of freedom in this investigation is taken to be one-third of the number of data points.

As may be seen by comparing Fig. 20a and Fig. 1a, significant correlation is found in the vicinity of the jet entrance longitudes, i.e., 20W-20E, 100E-130E and 140W-120W. The large correlation in 60E-90E is presumably due to the contribution from the second half of December when a jet maximum is found in a rather unclimatological position of 80E to 100E, shown to be a response to the large increase in equatorial divergence discussed in Section IV. The most impressive correlation is found between 170E and 150W. An examination of Fig. 1a reveals that this is the decelerating region of the mean East Asia jet. On the monthly mean (Fig. 1b), a large convergence center dominates the tropics in these longitudes. This is identified with the Mid-Pacific trough discussed by Krishnamurti et al. (1973).

Consistent with the shift of the major velocity potential center from the maritime continent to the Indian Ocean in January (Fig. 2b), the correlation is most pronounced over the longitudes 50E to 60E (Fig. 20b). The midlatitude zonal wind in these longitudes does not show up as particularly strong in the monthly mean. However the accentuation of the westerly zonal wind can be seen in the short-period average (not shown).

The correlation over the maritime continent longitudes in January (Fig. 20b) is significant at the 5% level and not at 2.5% level. There are two correlation peaks showing up in the mid-Pacific longitudes. A relatively large peak is found in the North American jet entrance region.

In February, the correlation coefficients are lower. This may be due to the fact the major velocity potential centers were found in the southern hemisphere. Moving the band for averaging tropical velocity potential farther south did not improve the results appreciably.

To confirm the visual impression seen in the longitude time sections, that the jet accelerations were almost simultaneous with the tropical velocity potential enhancement, the time-lag correlation coefficient for each longitude is computed. Here, positive time lag (in units of half-days) with positive correlation means that the zonal westerly acceleration is leading the tropical velocity potential. The maxima are found to quite centrally located (Fig. 2la), meaning that no

systematic time lag could be resolved by using this data set. A similar calculation was also carried out for longitude lags. It is found that within the limits of the grid resolution, the correlation between tropical velocity potential and the midlatitude zonal wind is best when they are of the same longitudes. Similar calculation were also carried out for the southern hemisphere. Fig. 2lb shows the time lag correlation for the southern hemisphere, which indicates no significant correlation over the Asia-Pacific longitudes (significant correlation is indicated around 110W) consistent with the known fact that the summer hemisphere local Hadley cell is much weaker.

## VI. SUMMARY OF RESULTS AND CONCLUSIONS

The findings of this study may be summarized as follows:

1. A significant daily correlation was found between the enhancement of 200 mb tropical divergence or large-scale convection and the intensification of the midlatitude jet directly to the north. The shift of the large-scale tropical convective area to a position such as Indian Ocean in the episode D can bring about a significant longitudinal displacement of the East Asian jet streak. The correlation is attributed to the Coriolis torque on the poleward divergent flow ( $v_x$ ) initiated by tropical convection. The increase in divergent velocity at the jet latitude is being relayed from the tropics in time too short to be resolved by the 12-hourly data used. The fast response in itself underlines the transient nature of the interaction.
2. Based on space-lag correlation calculation, the tropical convective source seemed to be most effective in producing acceleration in the midlatitudes at the same longitudes as the convective areas.
3. The major contribution to the jet streak propagation downstream, following a monsoon cold surge or a tropical convective flare-up, seems to be the self-advection of the zonal wind, as the divergent center did not move significantly. This is also consistent with

the better correlation coefficients found by using  $du/dt$  instead of  $\partial u/\partial t$ .

4. Synoptic causes for all of the enhanced tropical divergence events have not been identified, such as the first two peaks in the zonal wind series of the maritime continent (Fig. 13) and the episode B in Fig. 6b. Nevertheless, causes for the major events in December have been found, with episodes A, C and D due to tropical storm activity and E (and partly D') due to cold surges. Since tropical storms should be considered as tropically-forced system when they are already well developed, the episodes A, C and D assert the point that the midlatitude jet intensifications were consequences rather than causes of the 200-mb tropical divergence events. In the event E where the convection is midlatitude-forced, the further strengthening of the midlatitude jets, in addition to the initial strengthening due to baroclinically induced secondary circulation in the vicinity of the jet entrance, formed the feedback part of the two-way interaction mechanism suggested by Chang and Lau (1980, 1982).
5. The mid-Pacific convergence area which may be identified with the mid-Pacific trough discussed by Krishnamurti et al. (1973) seems to be important not only to the east-west circulation but also forms the sinking arm of the reverse Hadley cell crucial to the deceleration of the East Asia jet. The results suggest a possible

sequence of events starting with a large-scale tropical convection followed by strengthening of the midlatitude jet and then enhanced downstream jet deceleration and deepening of the mid-Pacific trough.

6. Incidental to the results outlined above, the analyses also lend confidence to the usefulness of the daily model-independent divergence field computed by FNOC, at least at the 200 mb level. The results may have some forecasting implication for the mid-latitudes, as an enhanced jet implies increased baroclinicity which may, in turn, lead to development of disturbances.

FIGURE 1a: THE MONTHLY (DEC 83) MEAN VECTOR WIND.

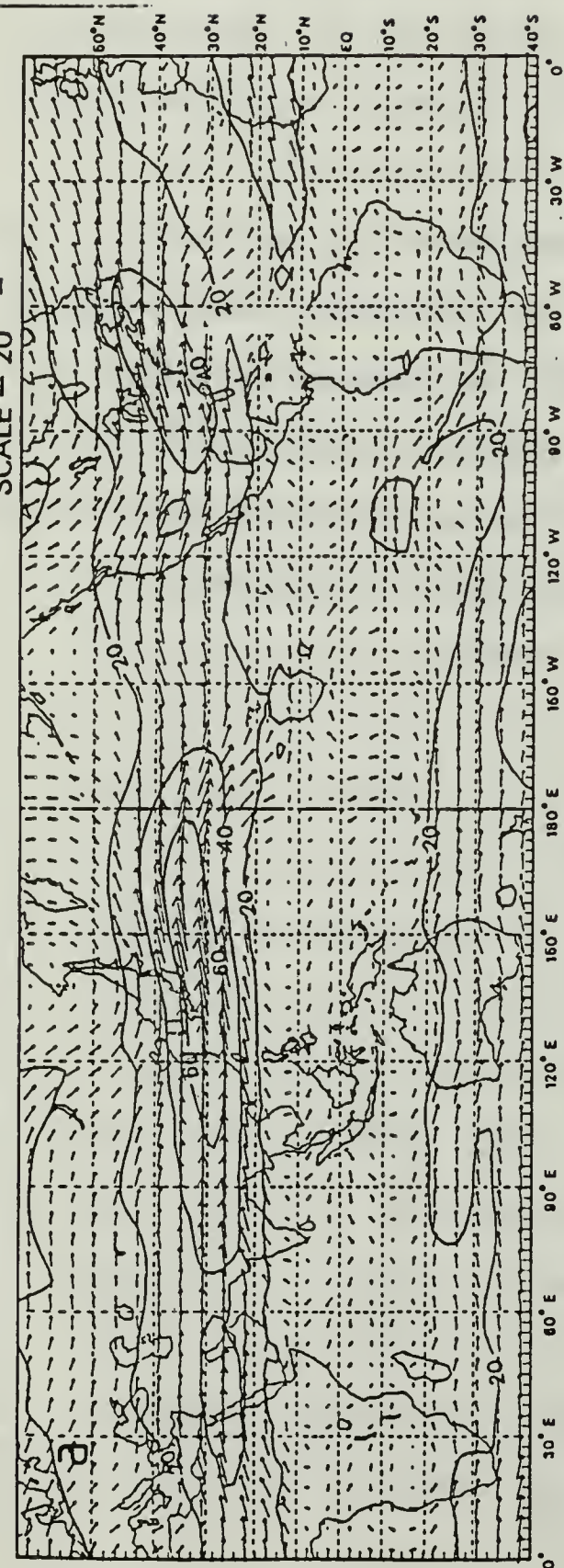


FIGURE 1b: THE MONTHLY (DEC 83) MEAN VELOCITY POTENTIAL.

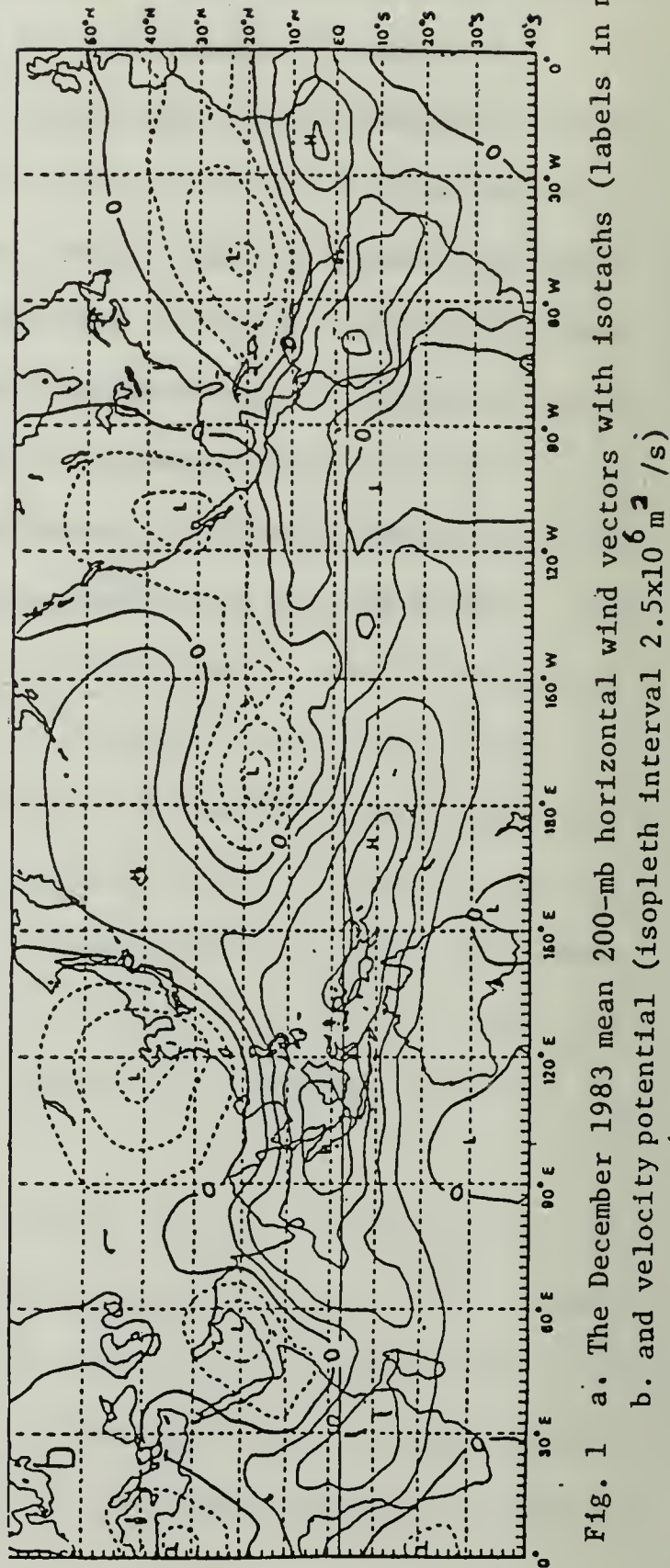


Fig. 1 a. The December 1983 mean 200-mb horizontal wind vectors with isotachs (labels in m/s)  
b. and velocity potential (isopleth interval  $2.5 \times 10^6 \text{ m}^2/\text{s}$ )

FIGURE 2a: THE MONTHLY (JAN 84) MEAN VECTOR WIND

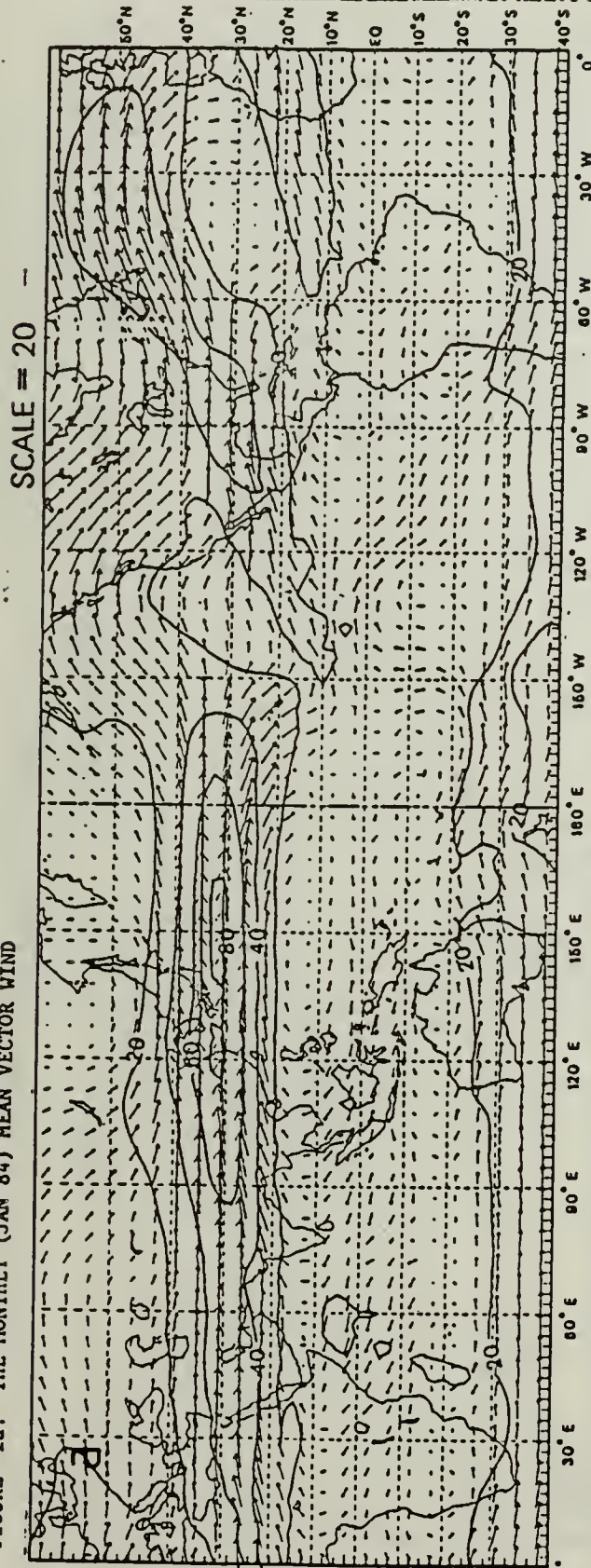


FIGURE 2b: THE MONTHLY (JAN 84) MEAN VELOCITY POTENTIAL

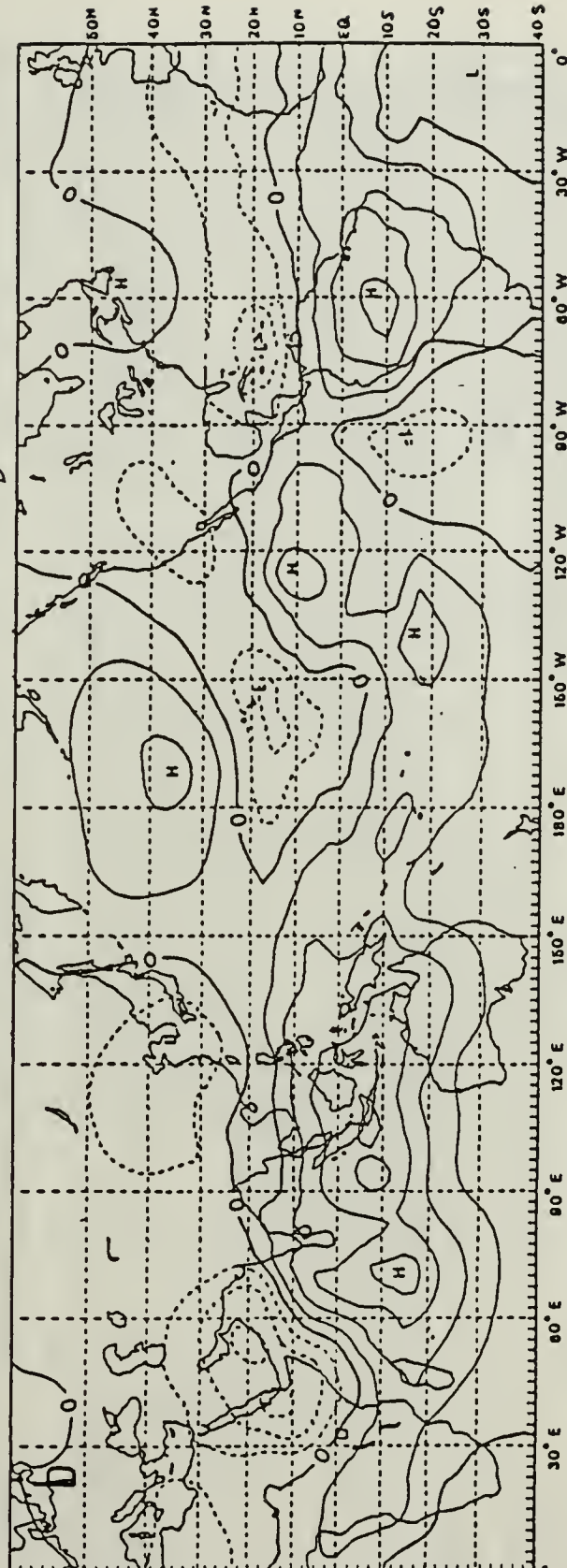


Fig. 2 As Fig. 1 except for January 1984.

FIGURE 3a: THE MONTHLY (FEB 84) MEAN VECTOR WIND

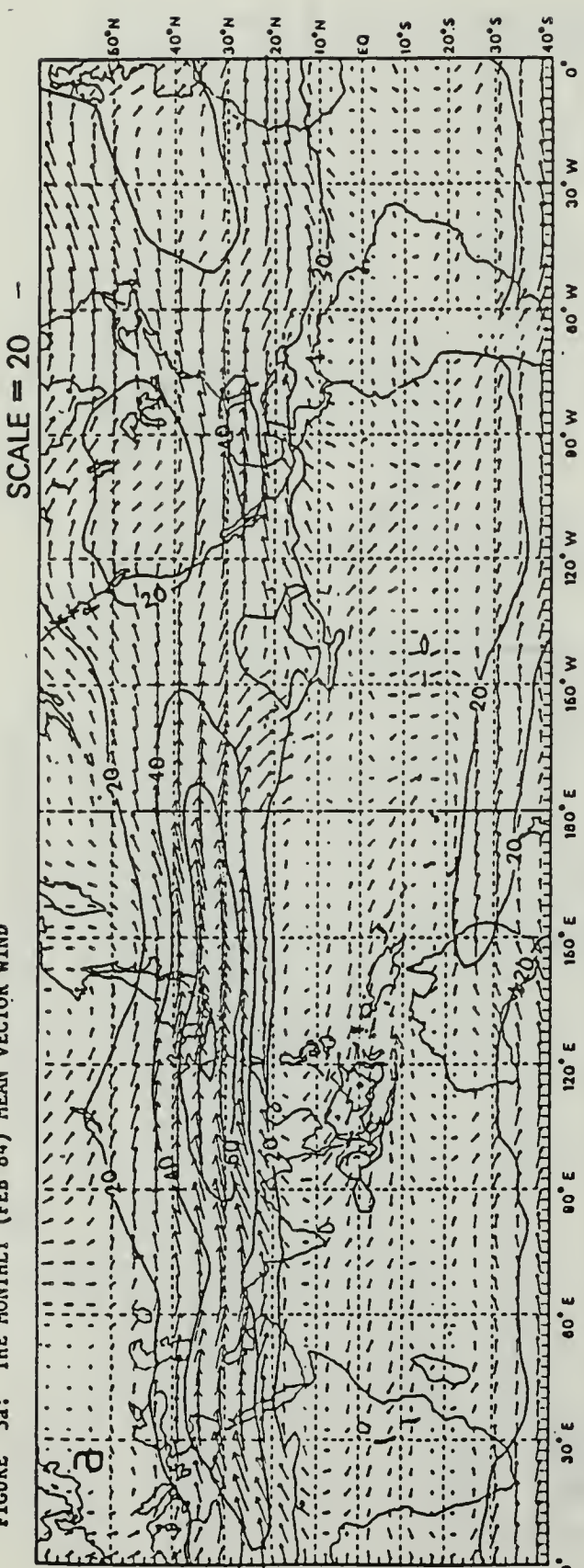


FIGURE 3b: THE MONTHLY (FEB 84) MEAN VELOCITY POTENTIAL

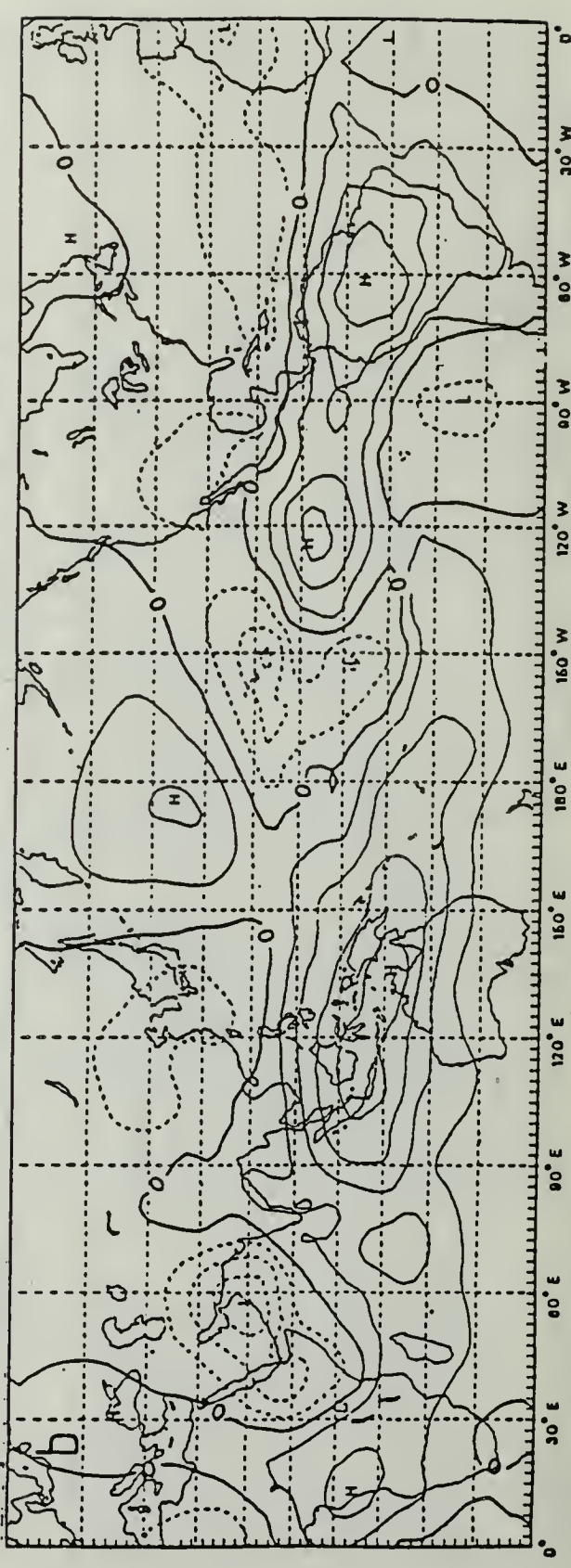


Fig. 3 As Fig. 1 except for February 1984.

FIGURE 4a: THE WINTER (1983/84) MEAN VELOCITY POTENTIAL

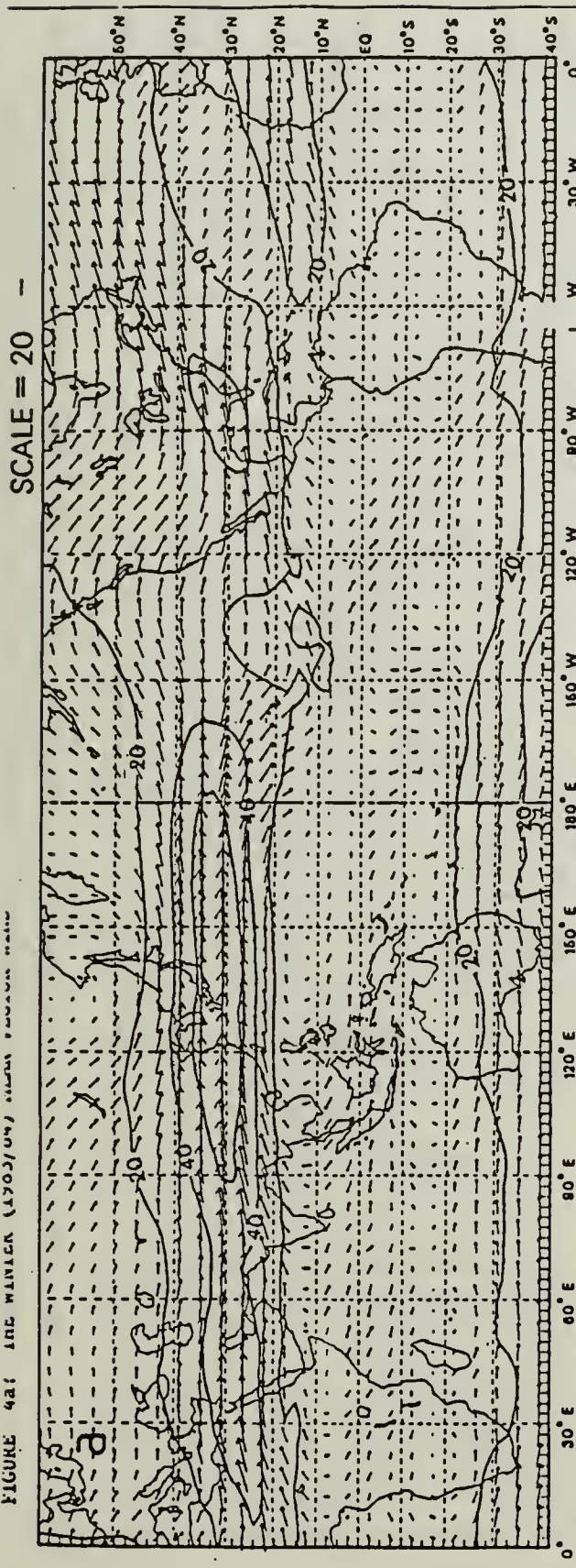


FIGURE 4b: THE WINTER (1983/84) MEAN VELOCITY POTENTIAL

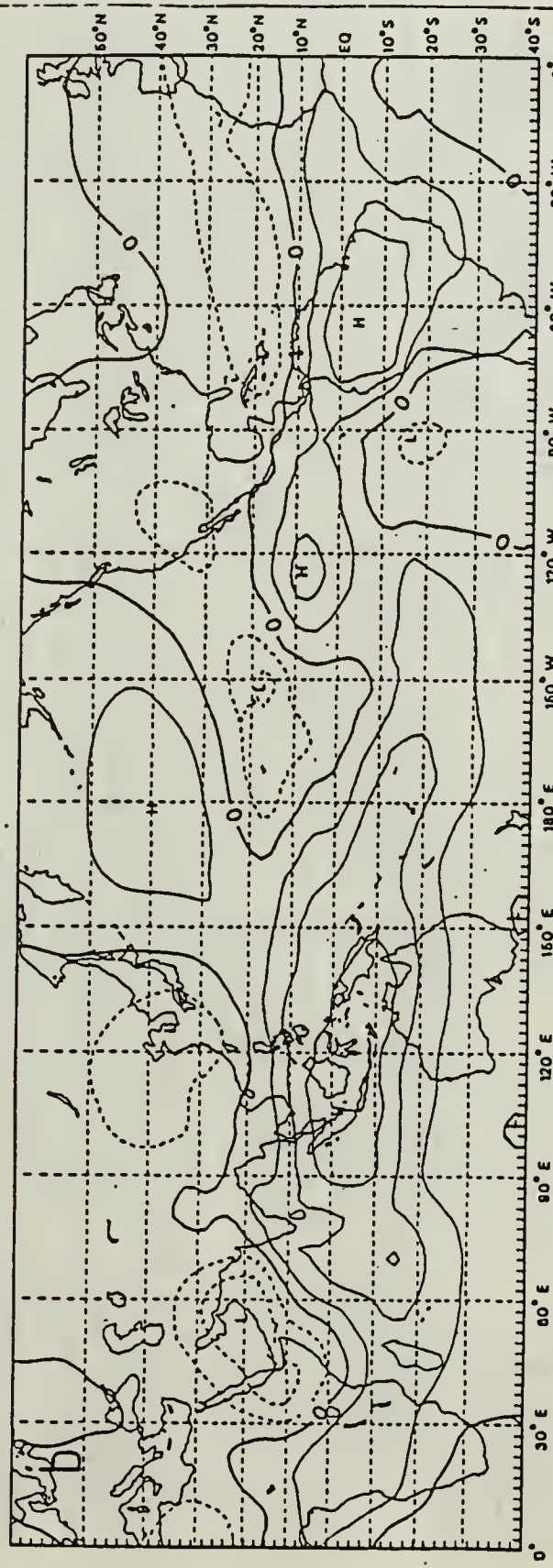


Fig. 4 As Fig. 1 except for the winter season 1983/84 (Dec 1983 – Feb 1984)

FIGURE 5a: VECTOR WIND FOR DAY 25 DEC 1983 (00 Z)

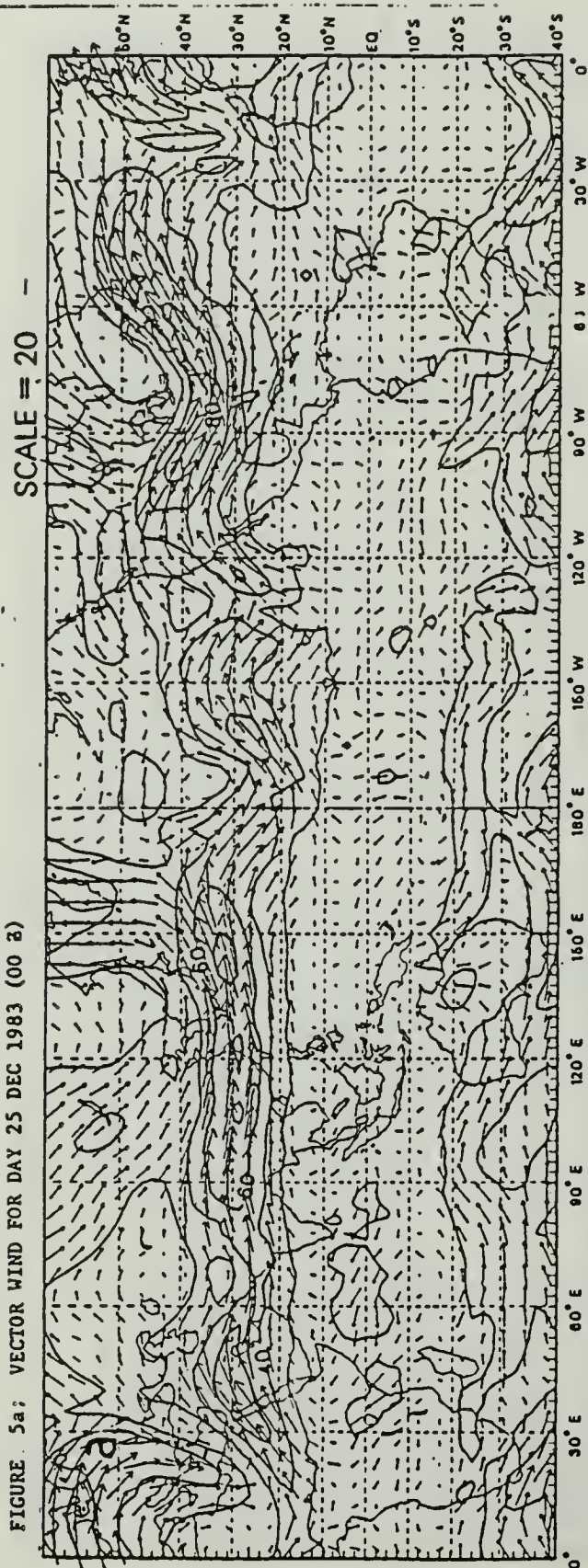


FIGURE 5a: VECTOR WIND FOR DAY 25 DEC 1983 (00 Z)

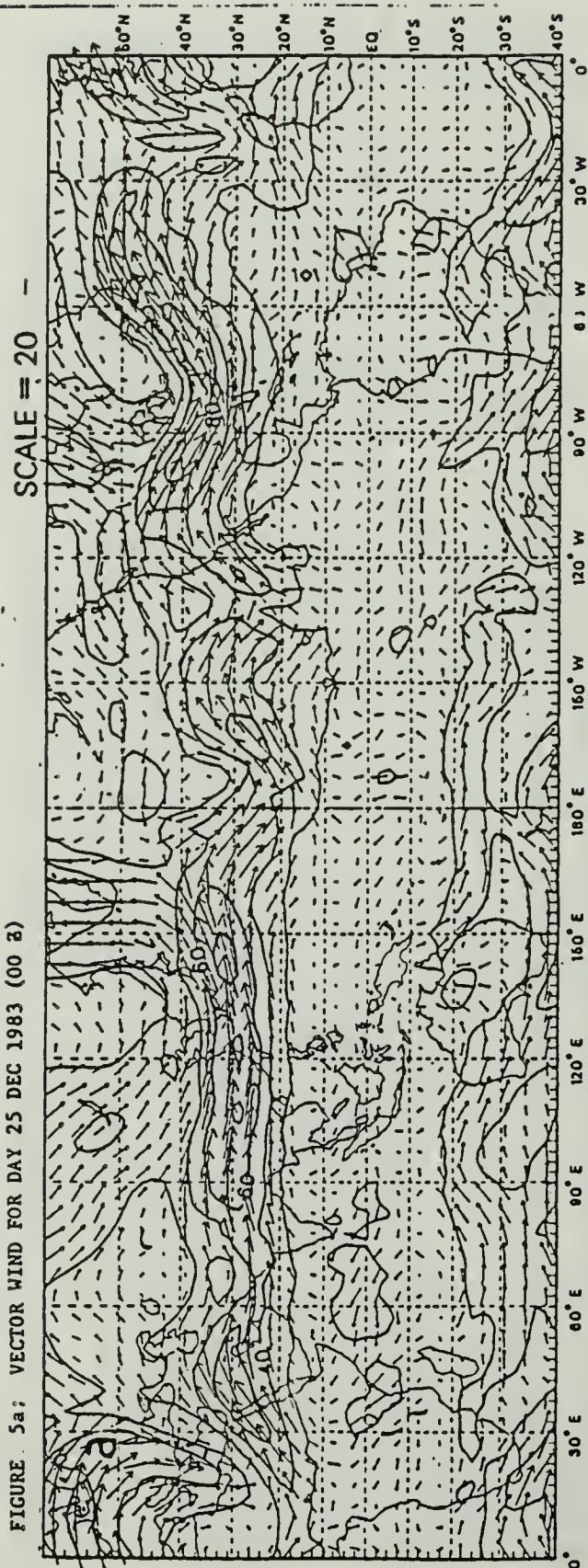


FIGURE 5b: VELOCITY POTENTIAL FOR DAY 25 DEC 1983 (00 Z)

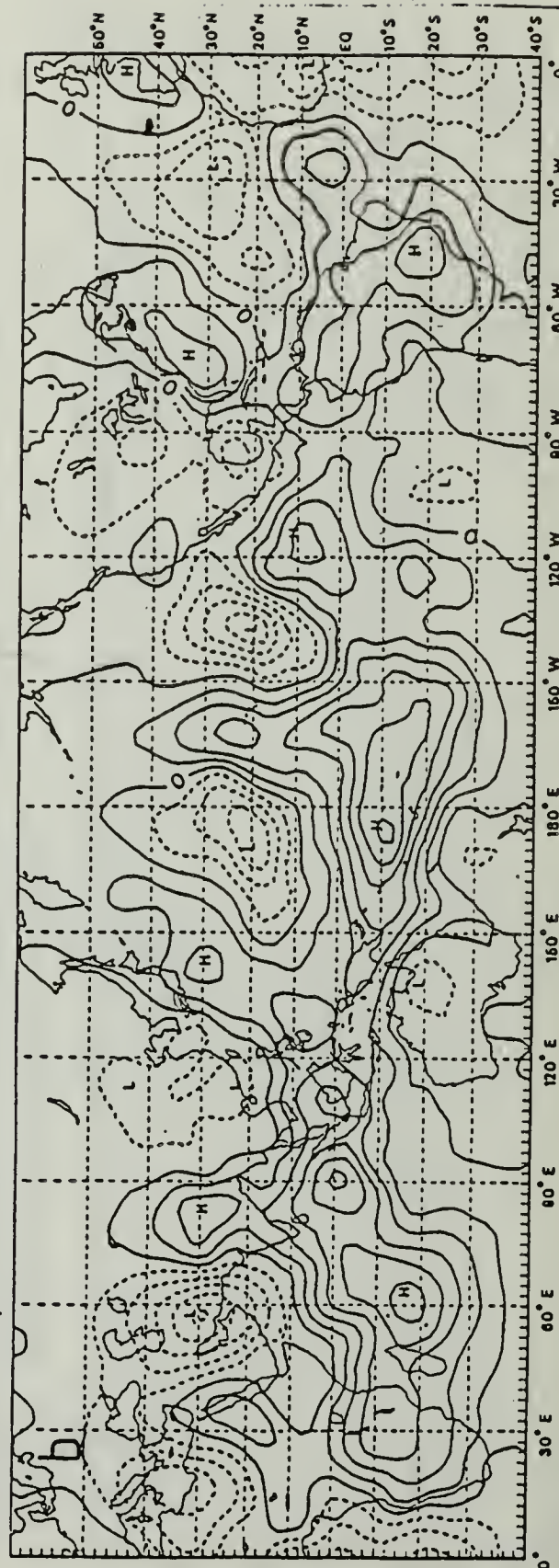


Fig. 5 a. The 200-mb horizontal wind vectors with isotachs (labels in m/s) for 25 Dec 1983  
 b. velocity potential (isopleth interval  $2.5 \times 10^{-6} \text{ m}^2/\text{s}$ ) for 25 Dec 1983 (00Z)

FIGURE 6a: LONG-TIME SECTION OF BAND (25N-40N) AVERAGED WESTERLY (DEC 1983)

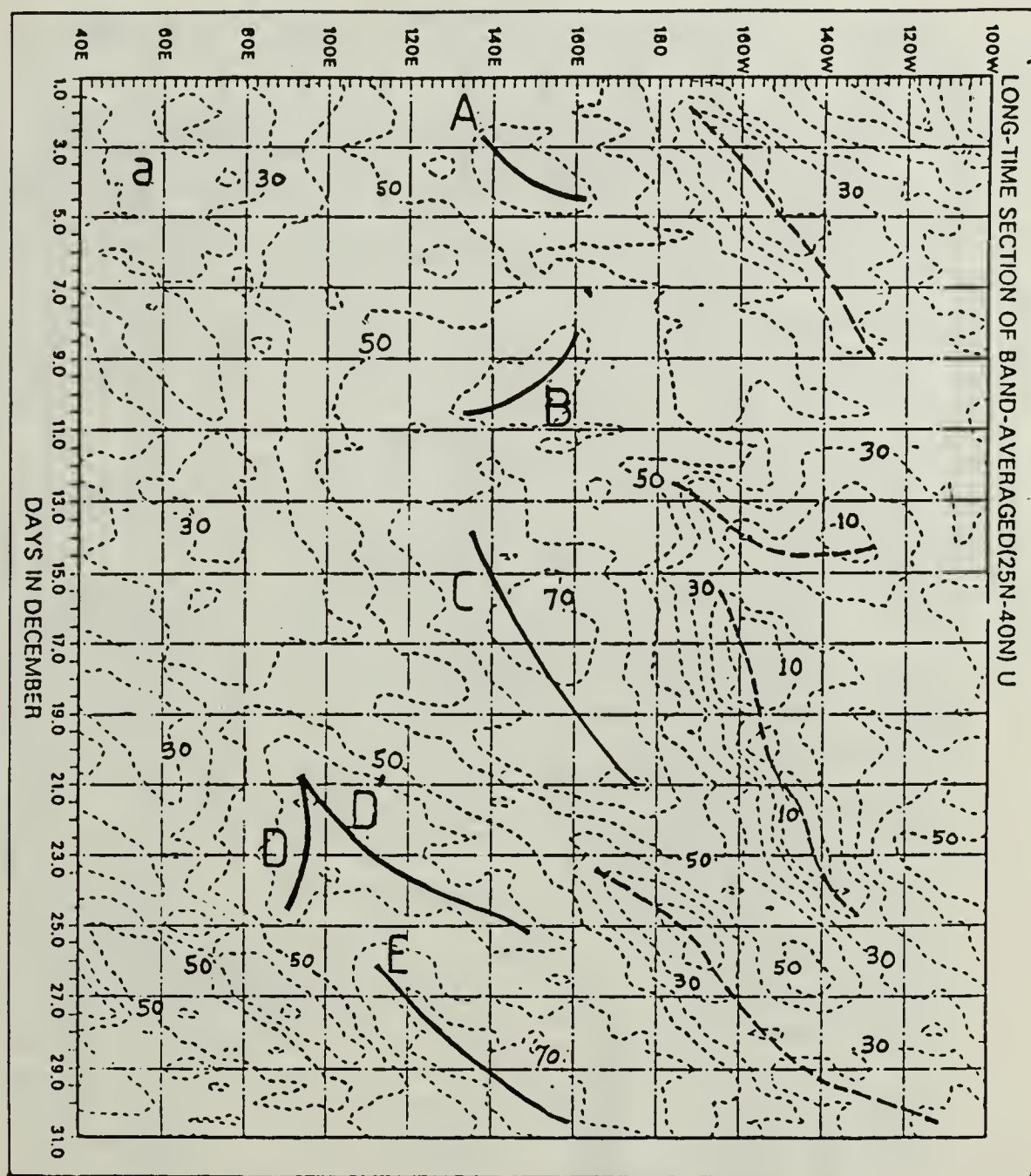


Fig. 6a      Longitude-time section of midlatitude zonal velocity (interval 10 m/s) averaged over  $25^{\circ}$ - $40^{\circ}$ N for December. The axes of maxima and minima are denoted by dark solid and dashed lines, respectively. Letters A, B, C, D, D' and E identify significant events of jet strengthening.

FIGURE 6b: LONG-TIME SECTION OF BAND (EQ-18N) AVERAGED VELOCITY POTENTIAL

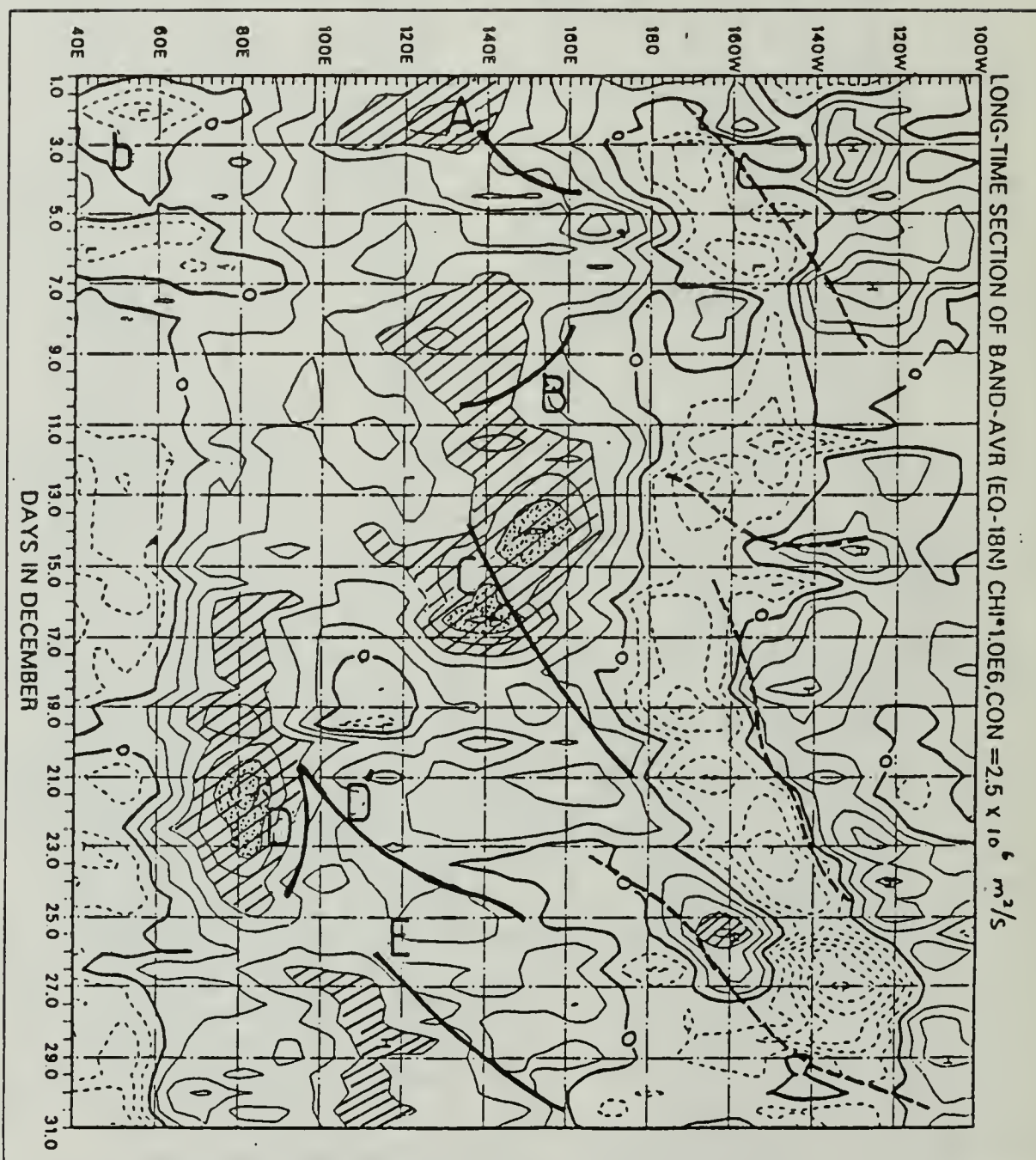


Fig. 6b      Longitude time section of tropical velocity potential (interval  $2.5 \times 10^6 \text{ m}^2/\text{s}$ ) averaged over  $0-18^\circ\text{N}$  of December with areas  $> 7.5 \times 10^6 \text{ m}^2/\text{s}$  hatched and area  $> 12.5 \times 10^6 \text{ m}^2/\text{s}$  are dotted. Dark solid and dashed lines indicating jet maxima and minima, respectively are copied from Fig. 6a.

FIGURE 7a: SAME AS FIG. 6a EXCEPT FOR JAN 84

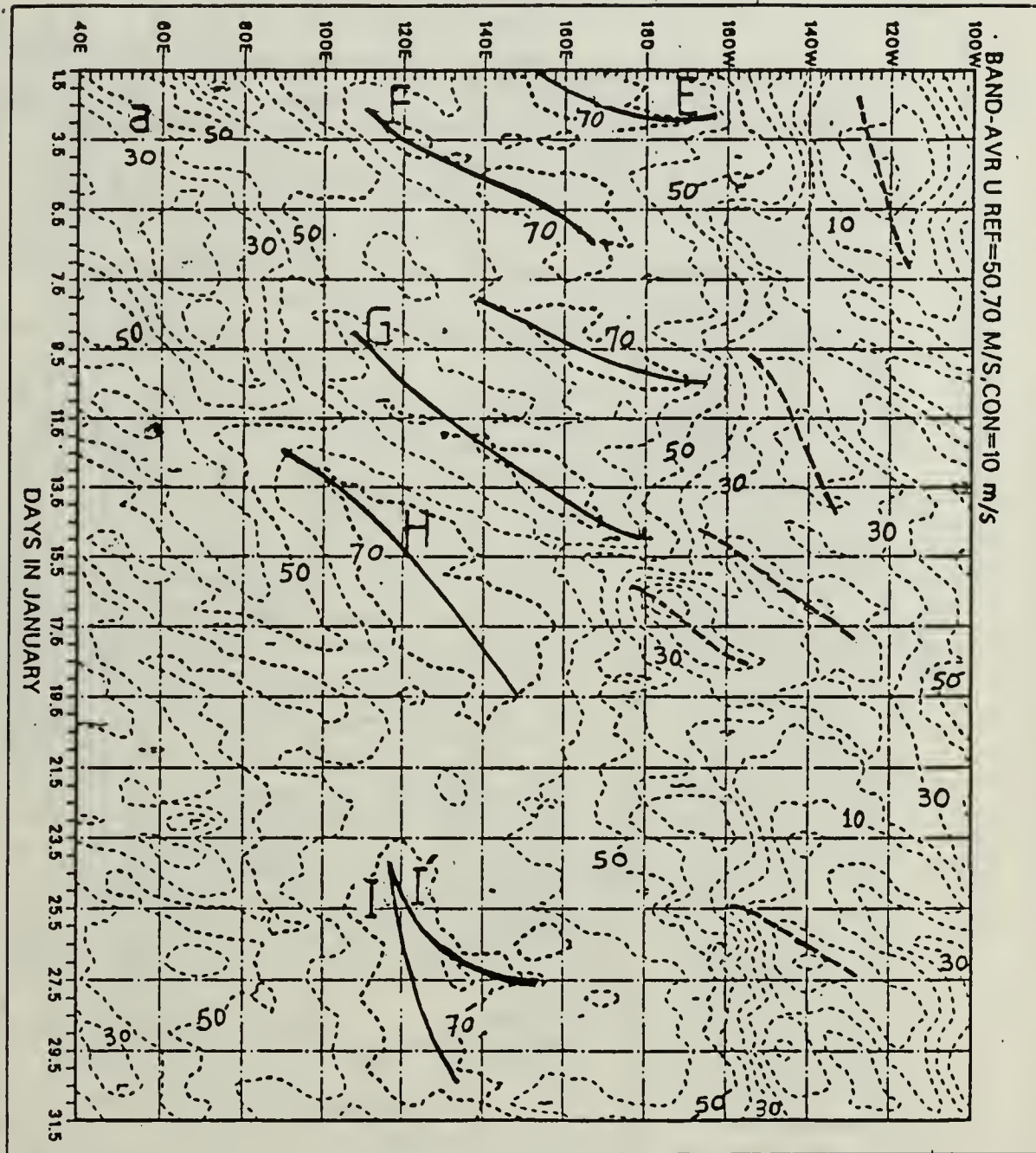


Fig. 7a Longitude-time section of midlatitude zonal velocity (interval 10 m/s) averaged over  $25^{\circ}$ - $40^{\circ}$ N for January. The axes of maxima and minima are denoted by dark and dashed lines, respectively.

FIGURE 7b: SAME AS FIG. 6a EXCEPT FOR JAN 84

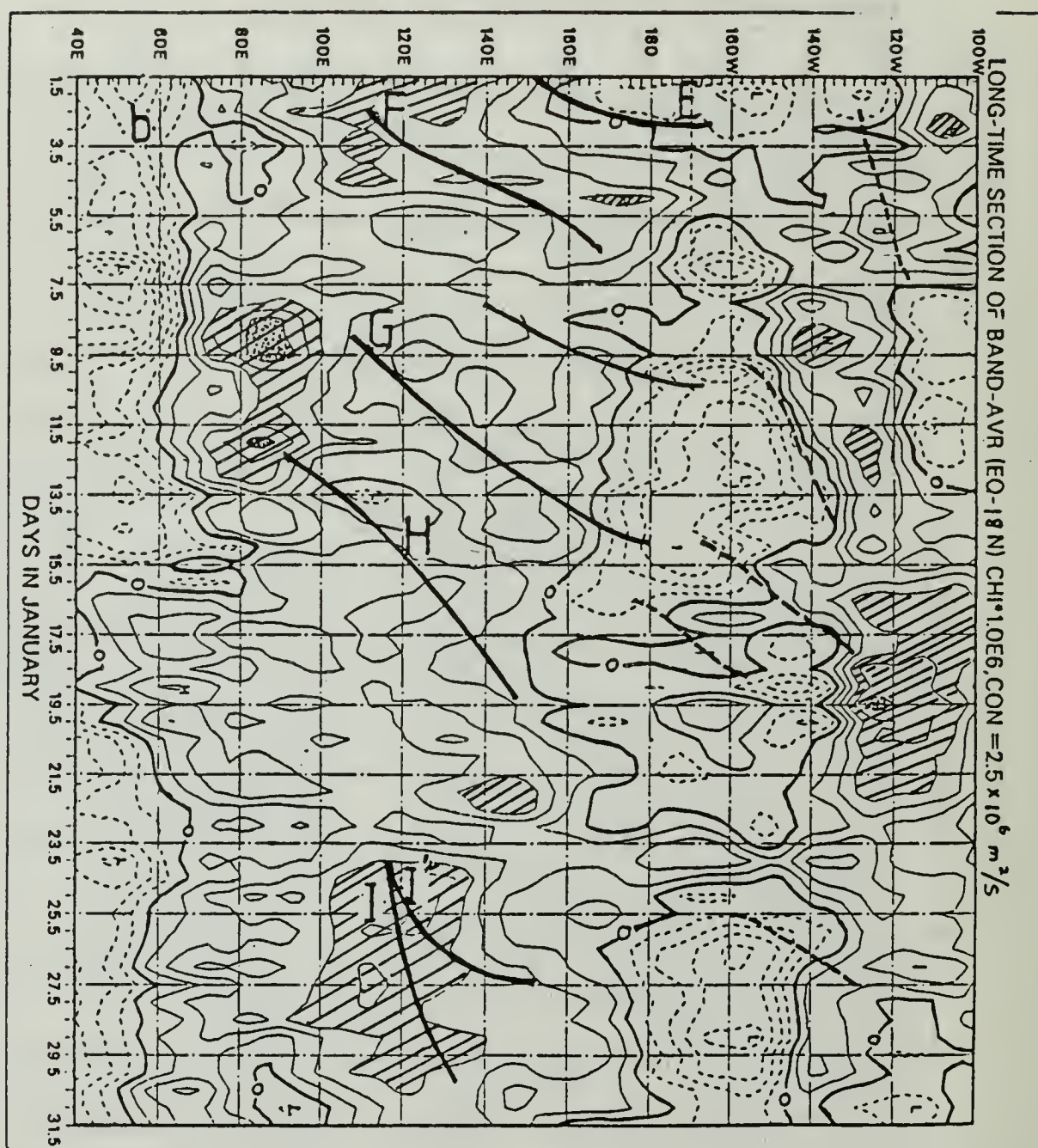


Fig. 7b     Longitude-time section of tropical velocity potential (interval  $2.5 \times 10^6 \text{ m}^2/\text{s}$ ) averaged over 0-18°N of January. With areas  $\geq 7.5 \times 10^6 \text{ m}^2/\text{s}$  hatched and area  $\geq 12.5 \times 10^6 \text{ m}^2/\text{s}$  dotted. Dark solid and dashed lines indicating jet maxima and minima, respectively are copied from Fig. 7a.

FIGURE 8a: SAME AS FIG. 6a EXCEPT FOR FEB 84

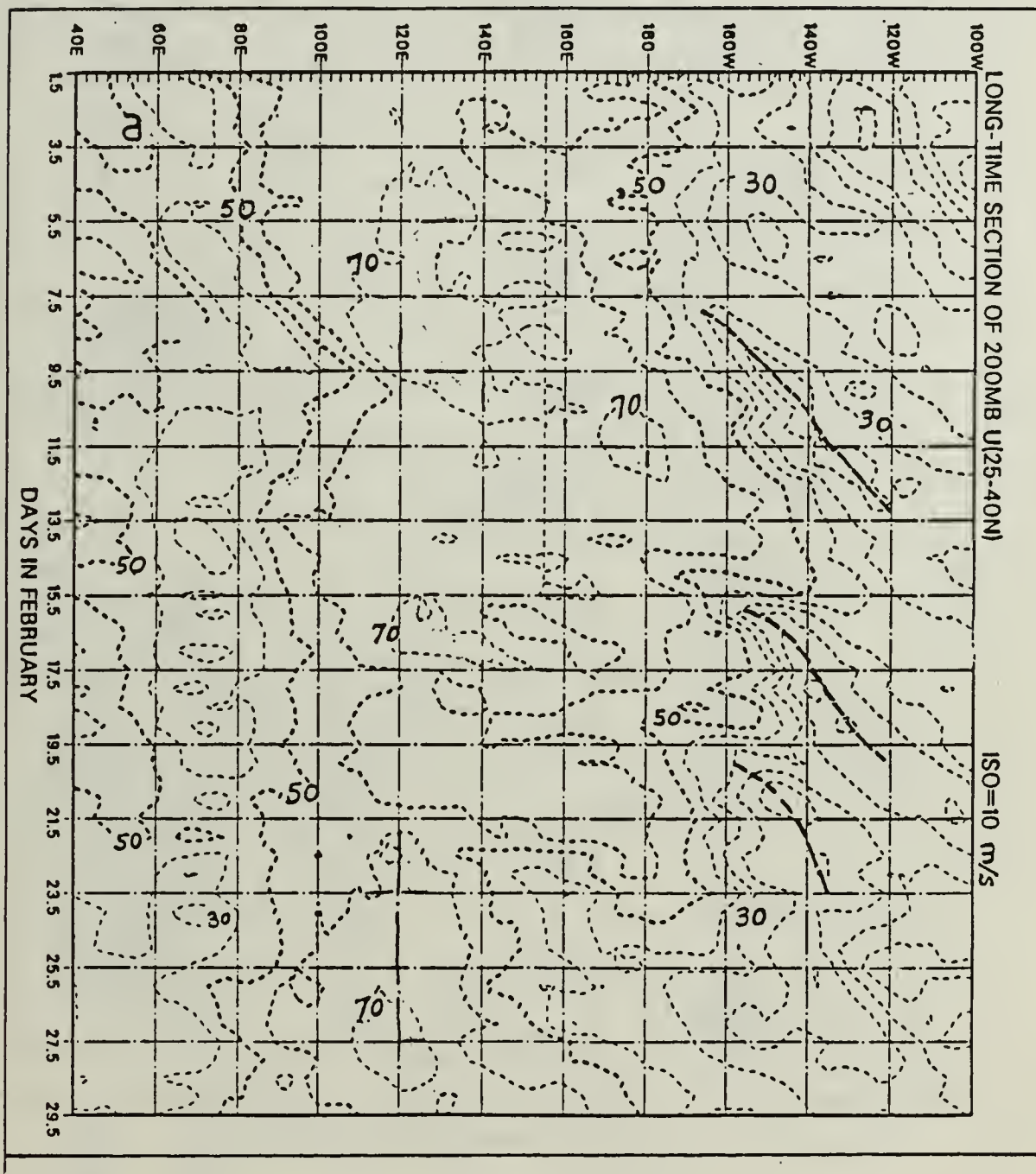


Fig. 8a As Fig. 7a except for February.

FIGURE 8b: SAME AS FIG. 6b EXCEPT FOR FEB 84

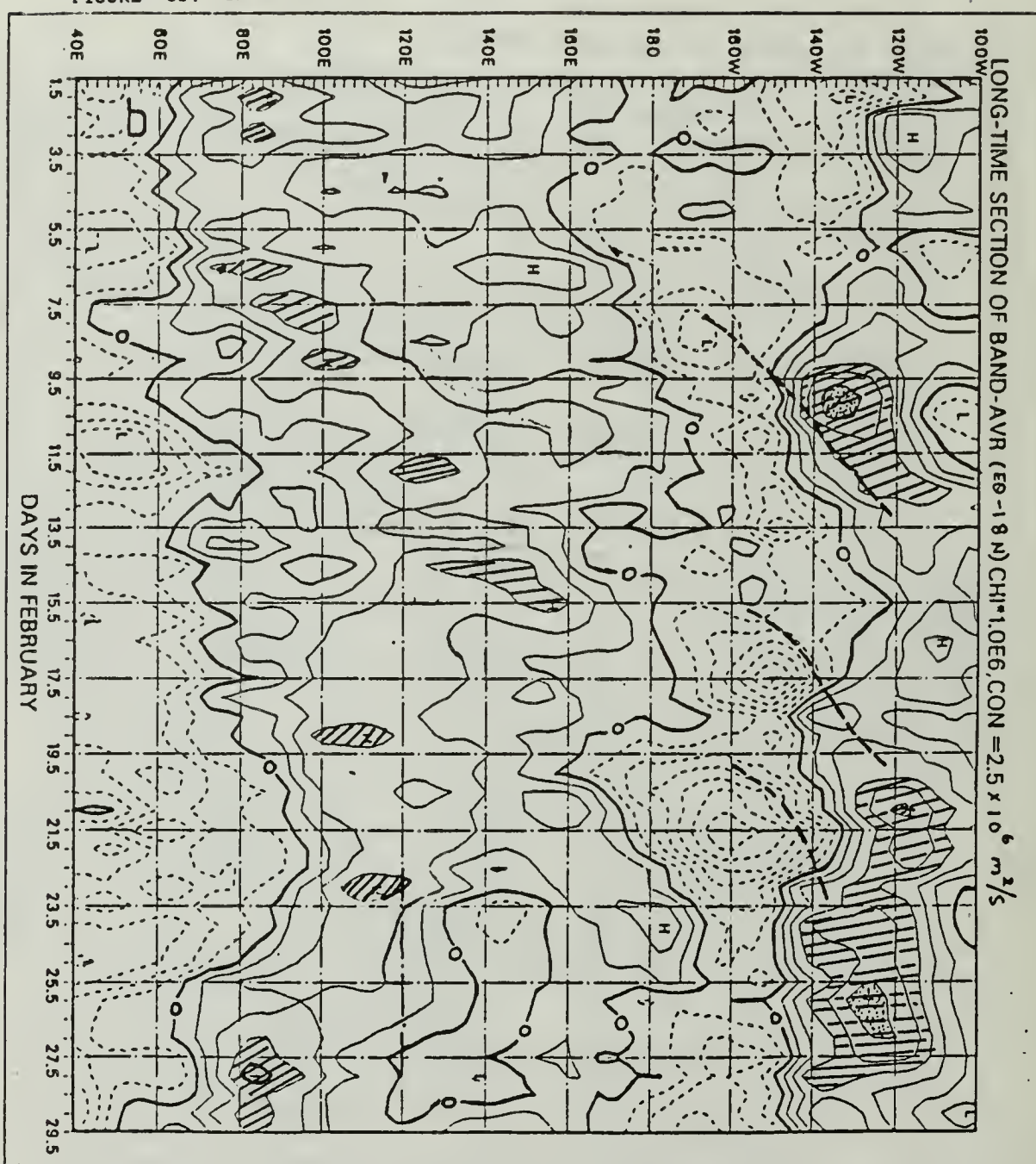


Fig. 8b As Fig. 7b except for February.

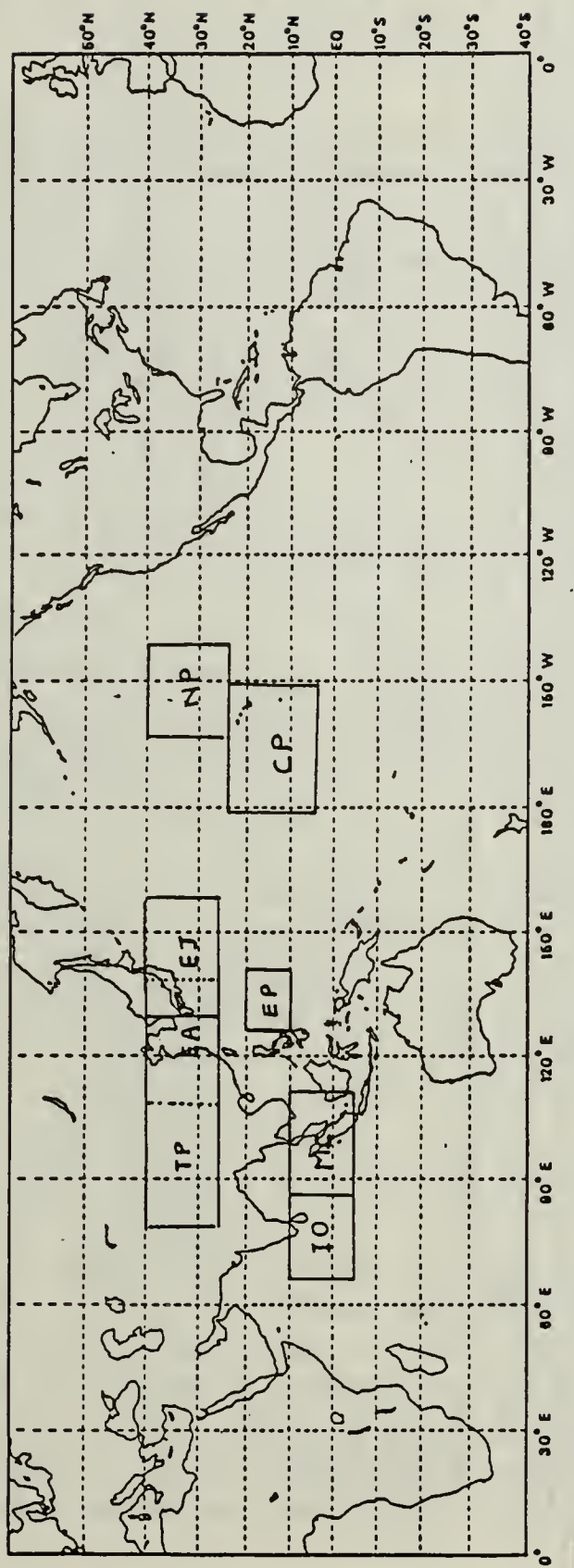


Fig. 9 Locations of areas for averaging zonal velocity and tropical divergence.

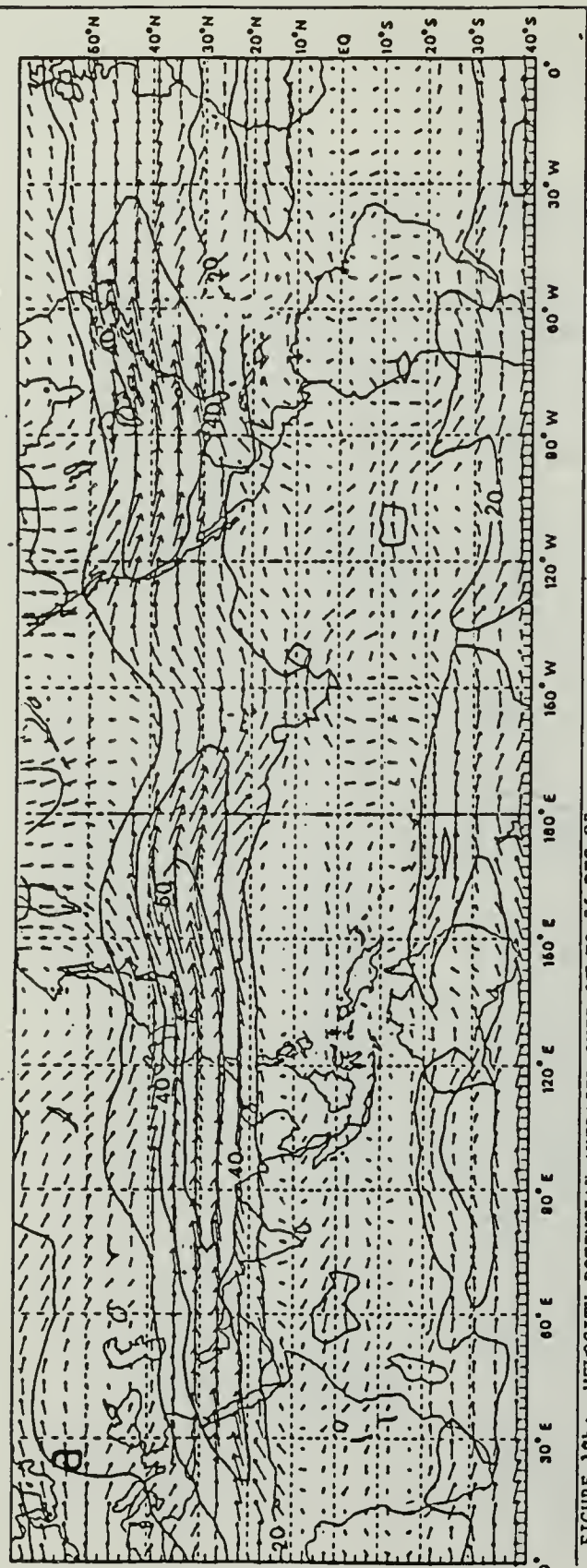


FIGURE 10b: VELOCITY POTENTIAL AVERAGED OVER 17 TO 26 DEC 83

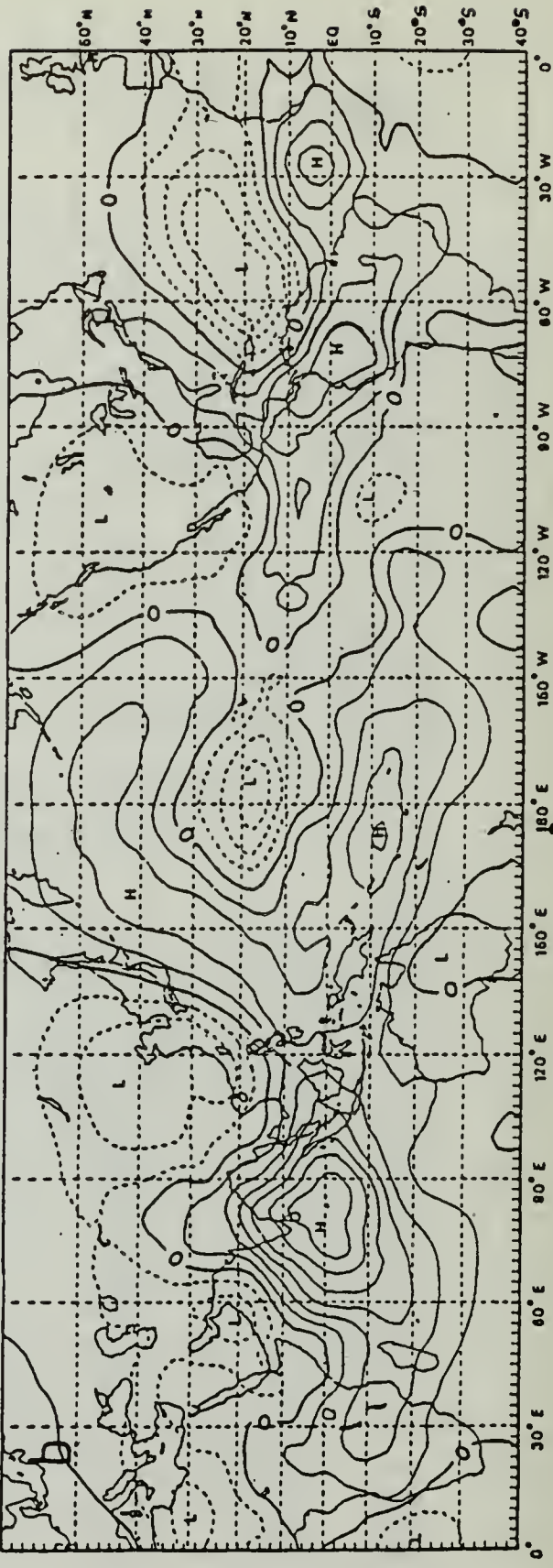


Fig. 10 As Fig. 1 except for the period 17-26 December 1983.

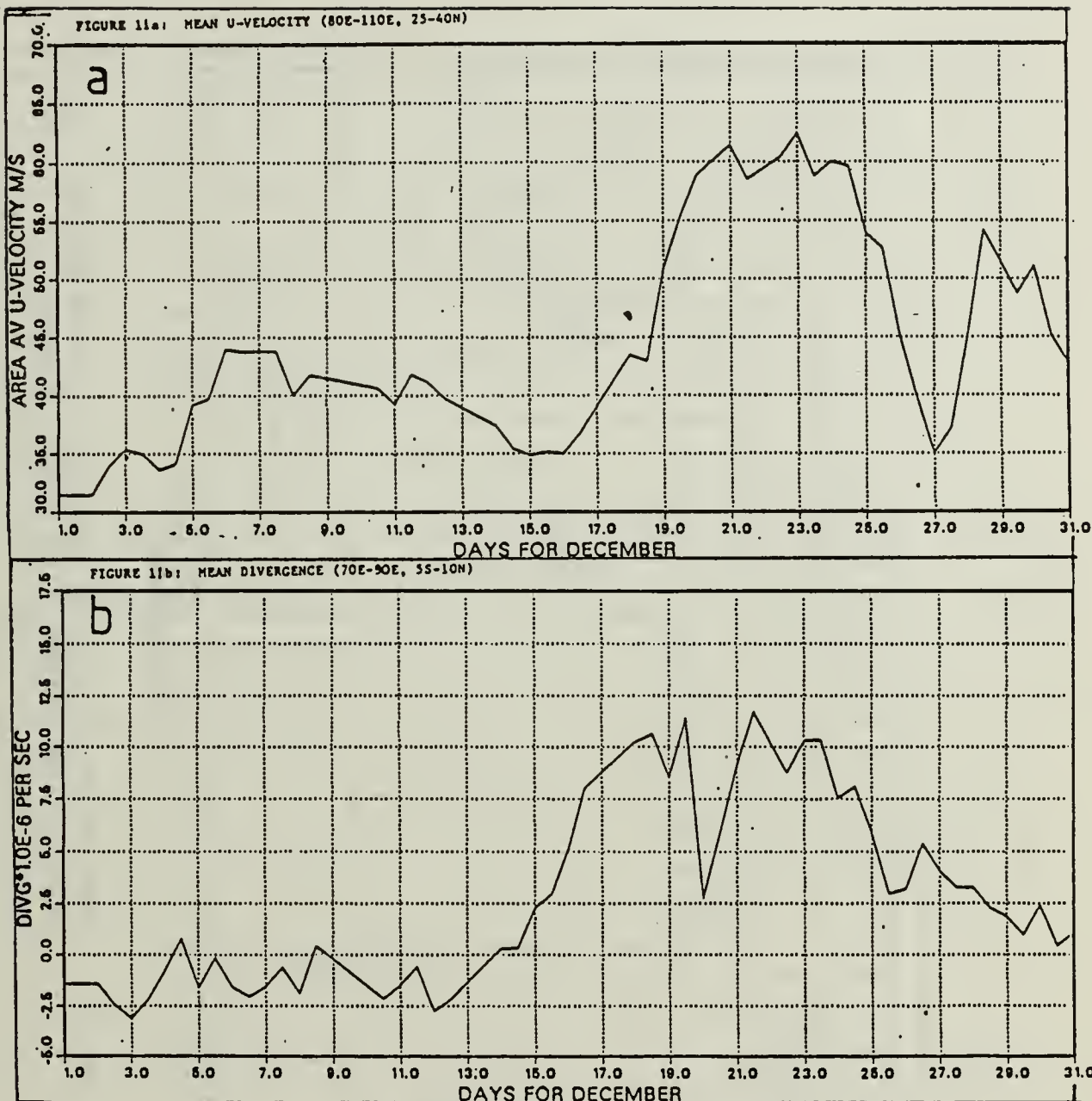


Fig. 11a Time series of area-averaged zonal velocity for the Tibetan Plateau region, (TP) ( $80^{\circ}$ - $110^{\circ}$ E,  $25$ N- $40$ N)

Fig. 11b Time series of area-averaged horizontal divergence for the equatorial Indian Ocean region (IO) ( $70^{\circ}$ - $90^{\circ}$ E,  $5$ S- $10$ N)

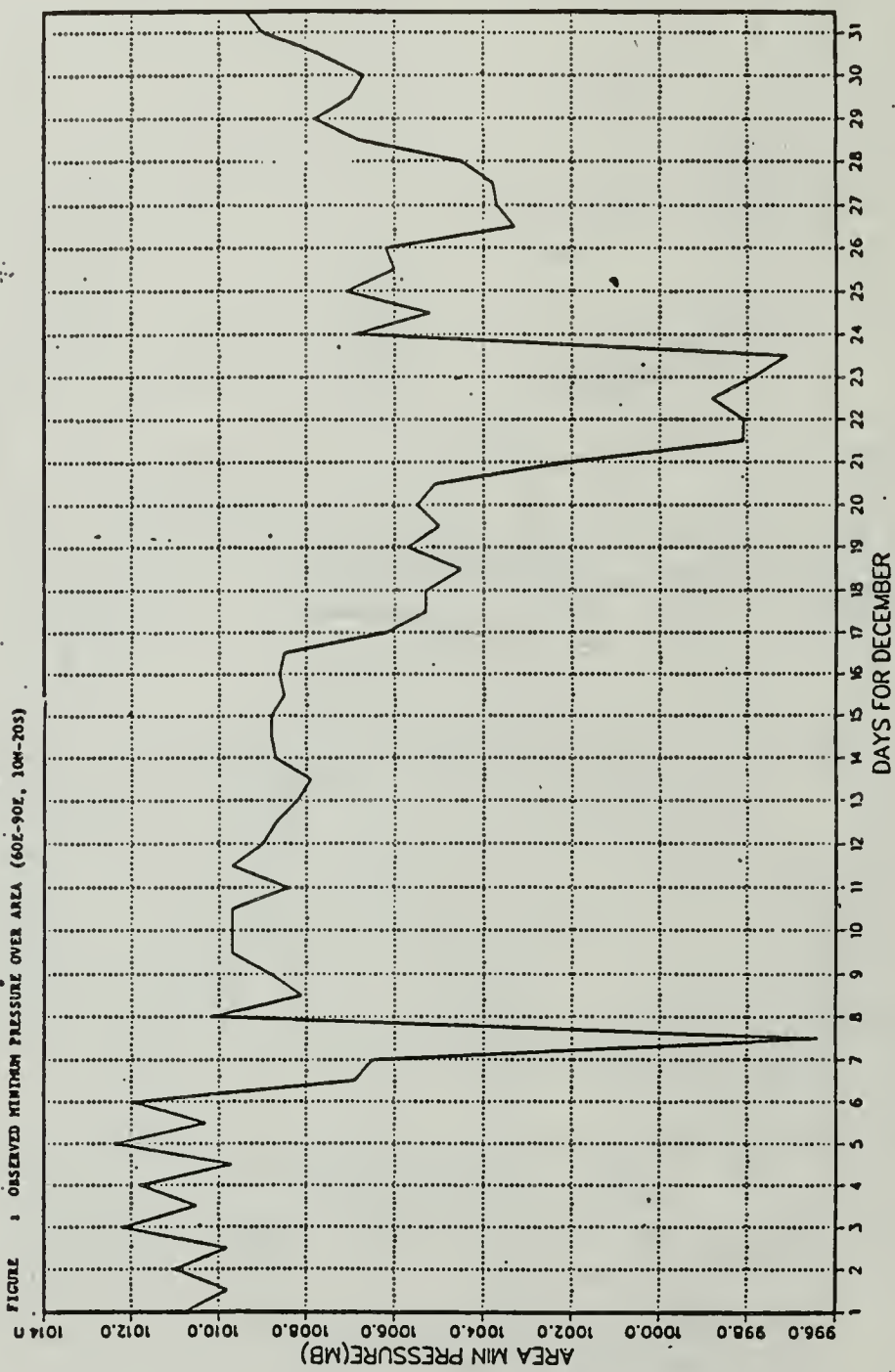


Fig. 12 Time series of minimum reported pressure in the Indian Ocean region of  $60^{\circ}$ - $90^{\circ}$  E, 20S-10N

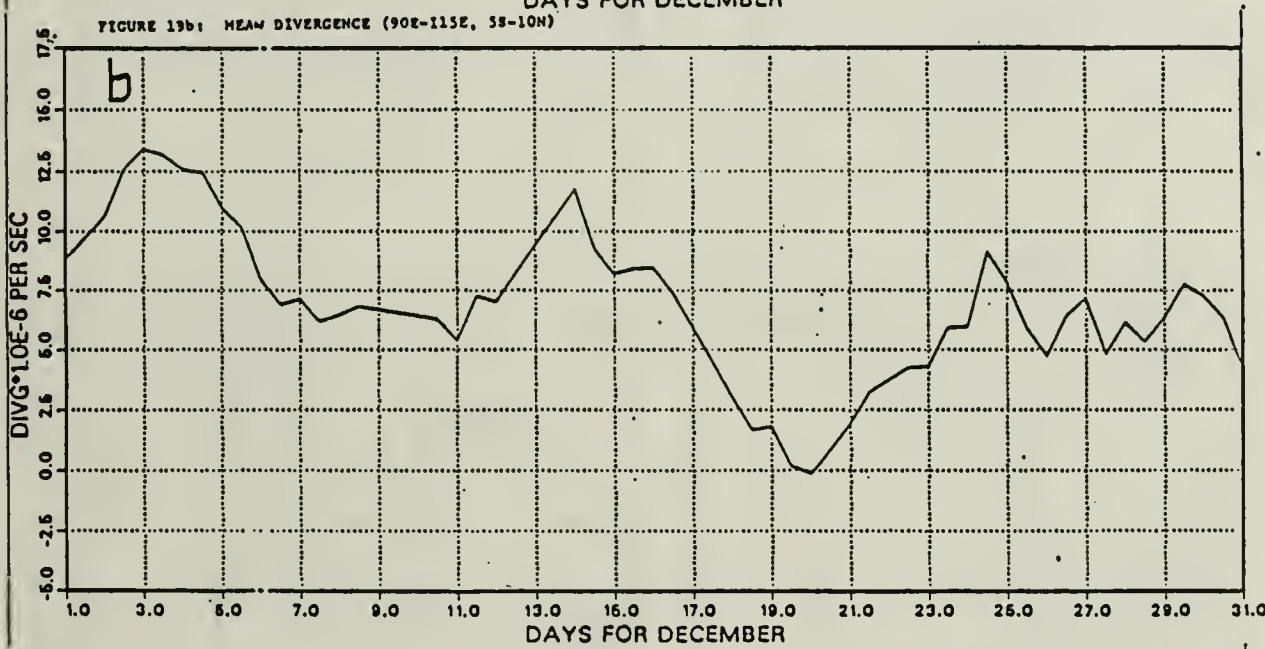
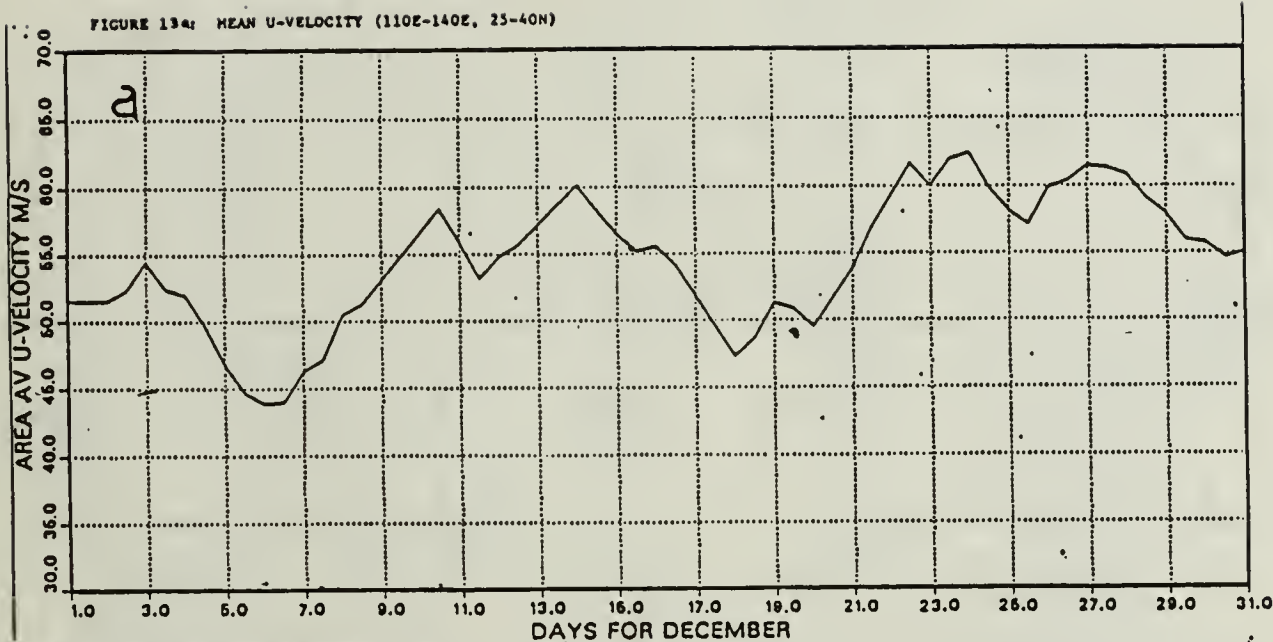
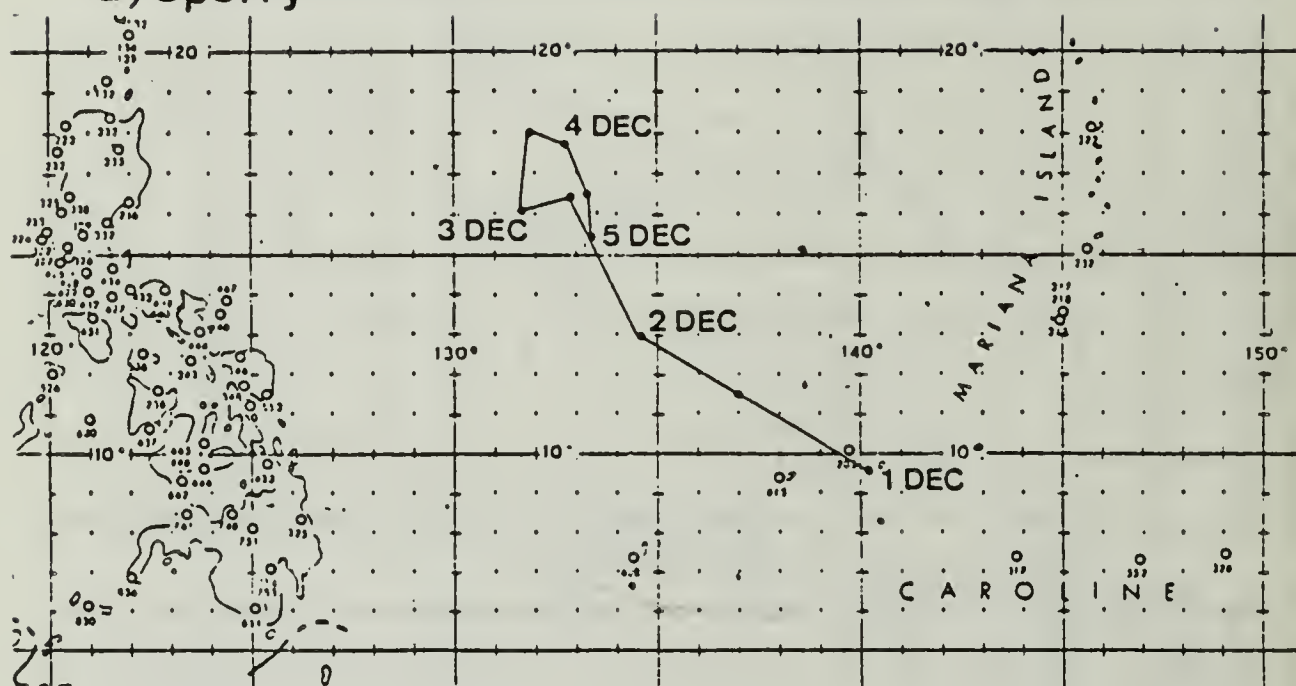


Fig. 13a As in Fig. 11a except for the East Asia-western Pacific region (EA) ( $110^{\circ}$ - $140^{\circ}$ E,  $25^{\circ}$ - $40^{\circ}$ N)

Fig. 13b As in Fig. 11b except for maritime continent (MC) region ( $90^{\circ}$ - $115^{\circ}$ E,  $5^{\circ}$ S- $10^{\circ}$ N)

a) Sperry



b) Thelma

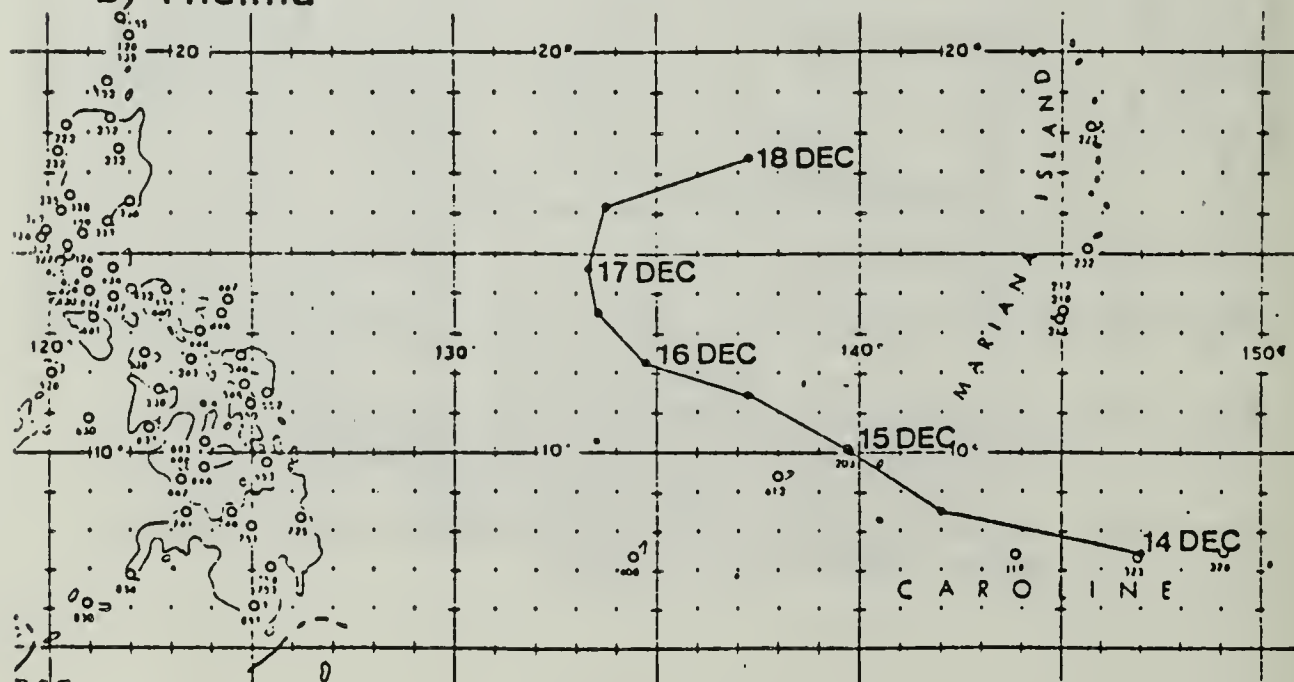


Fig. 14      Storm tracks for (a) Sperry and (b) Thelma 1983.

FIGURE 15c: VECTOR WIND AVERAGED OVER 14 TO 18 DEC 83

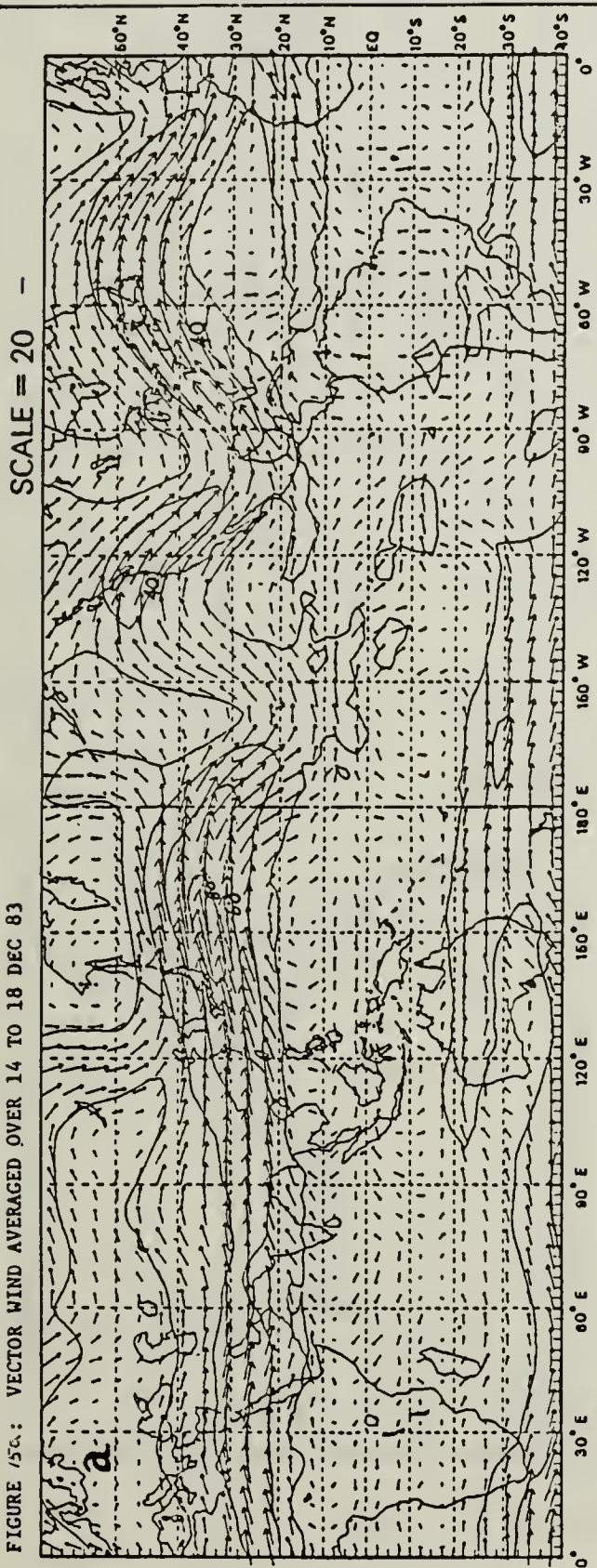


FIGURE 15b : VELOCITY POTENTIAL AVERAGED OVER 14' TO 18 DEC 83

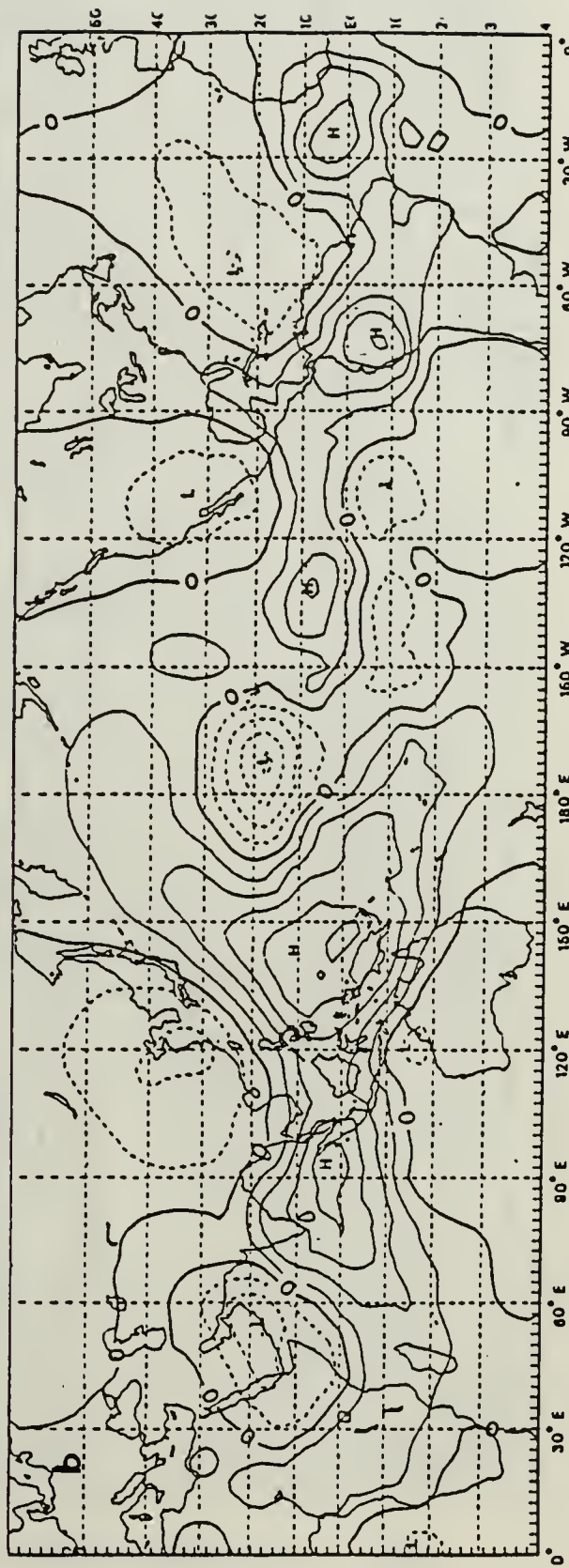


Fig. 15 As Fig. 1 except for the period 14-18 Dec 1984.

FIGURE 16A : VECTOR WIND AVERAGED OVER 1 TO 5 DEC 83

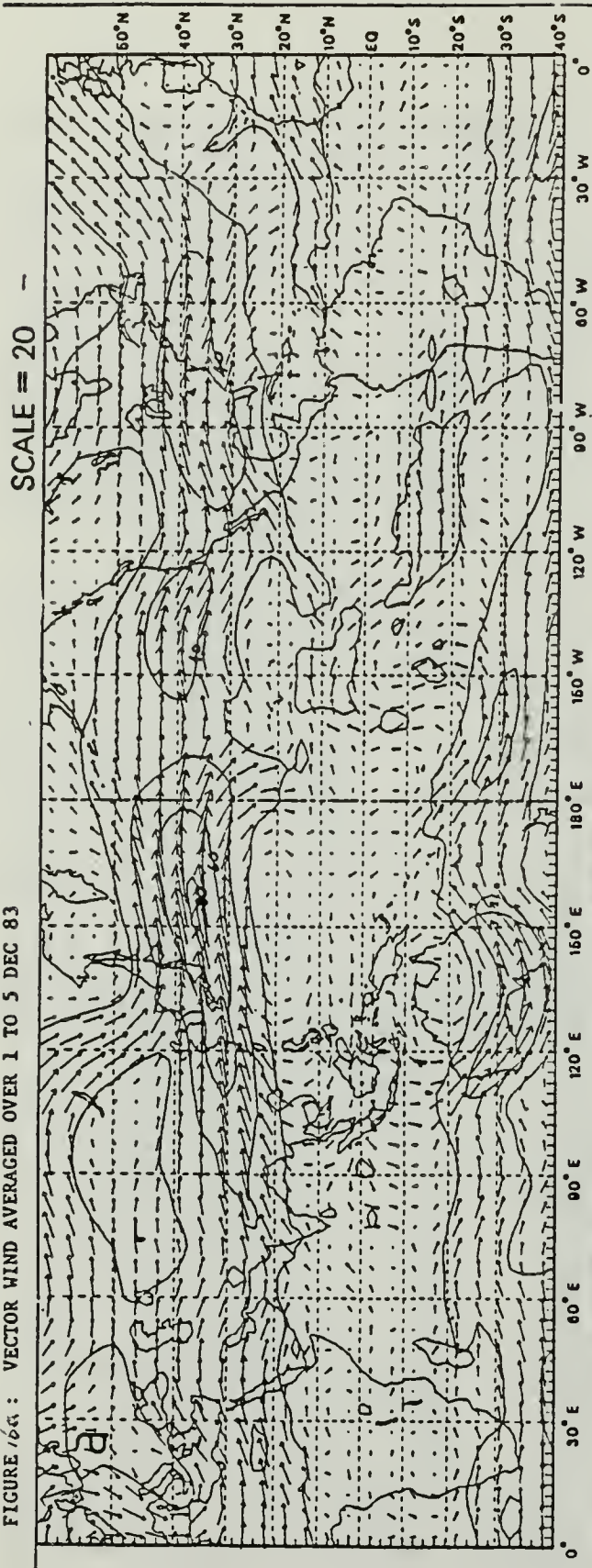
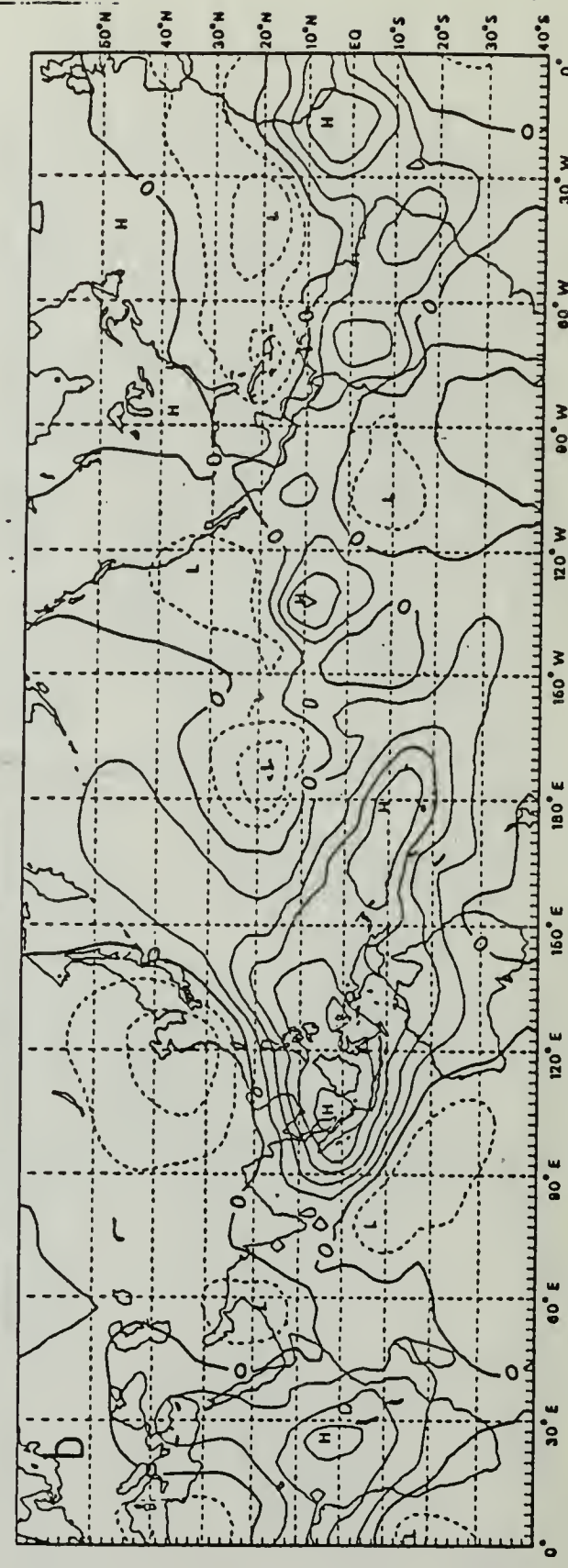
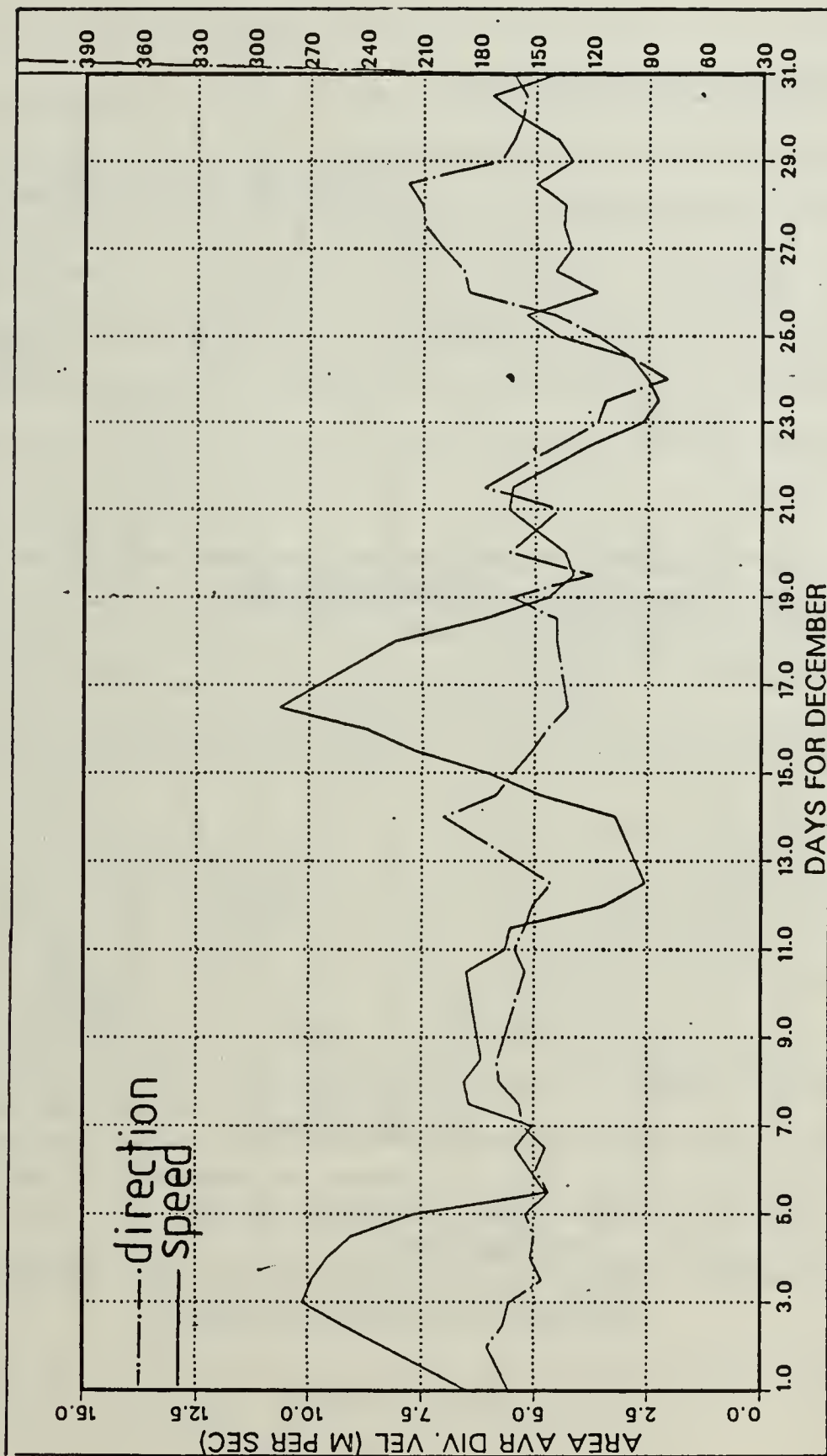


FIGURE 16B : VELOCITY POTENTIAL AVERAGED OVER 1 TO 5 DEC 83



• Fig. 16 As Fig. 1 except for the period 1-5 Dec. 1984.



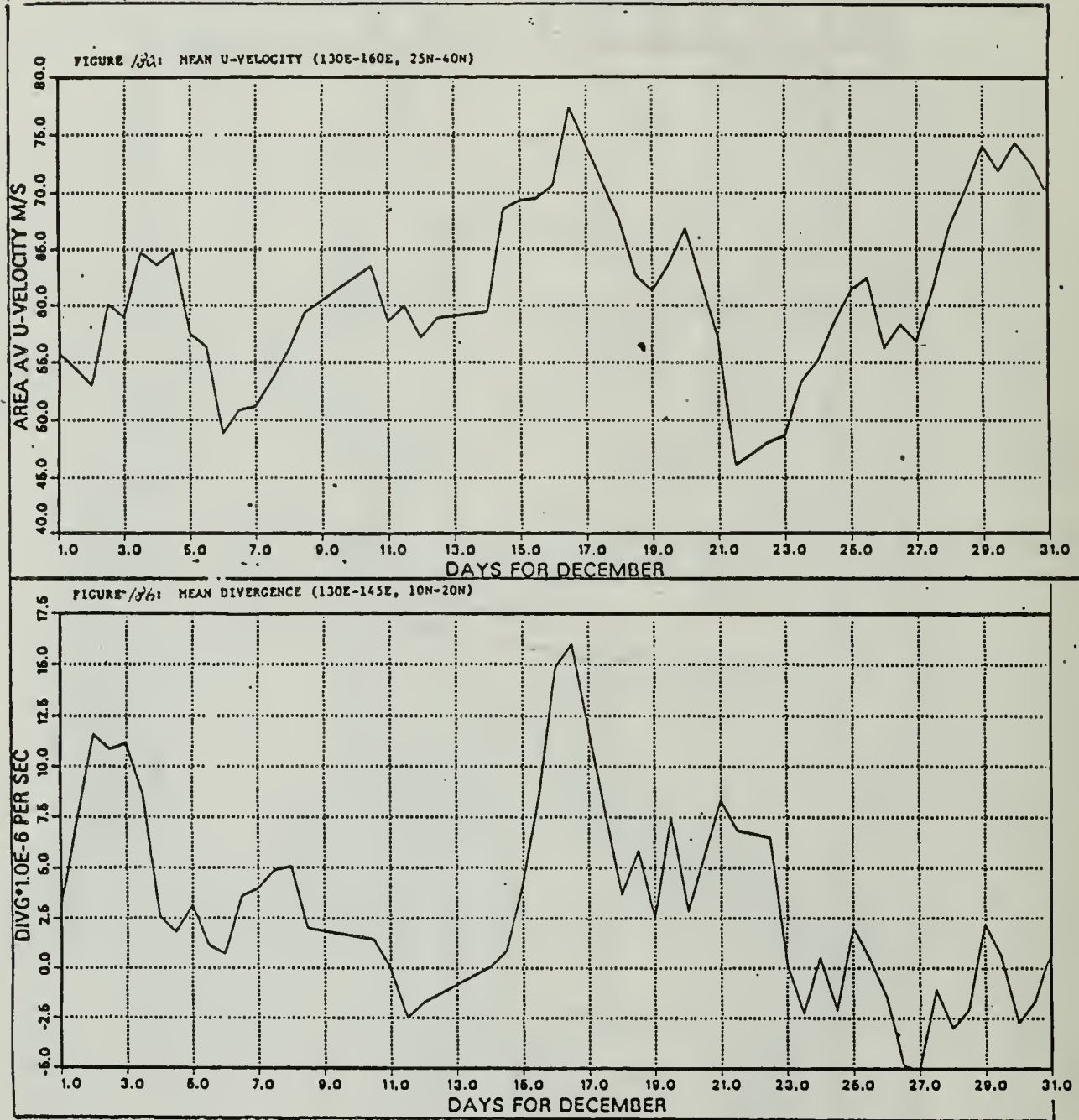


Fig. 18a As in Fig. 11a except for the East of Japan region (EJ) (130-160E, 25-40N)

Fig. 18b As in Fig. 11b except for the East of Philippines region (EP) (130-145E, 10-20N)

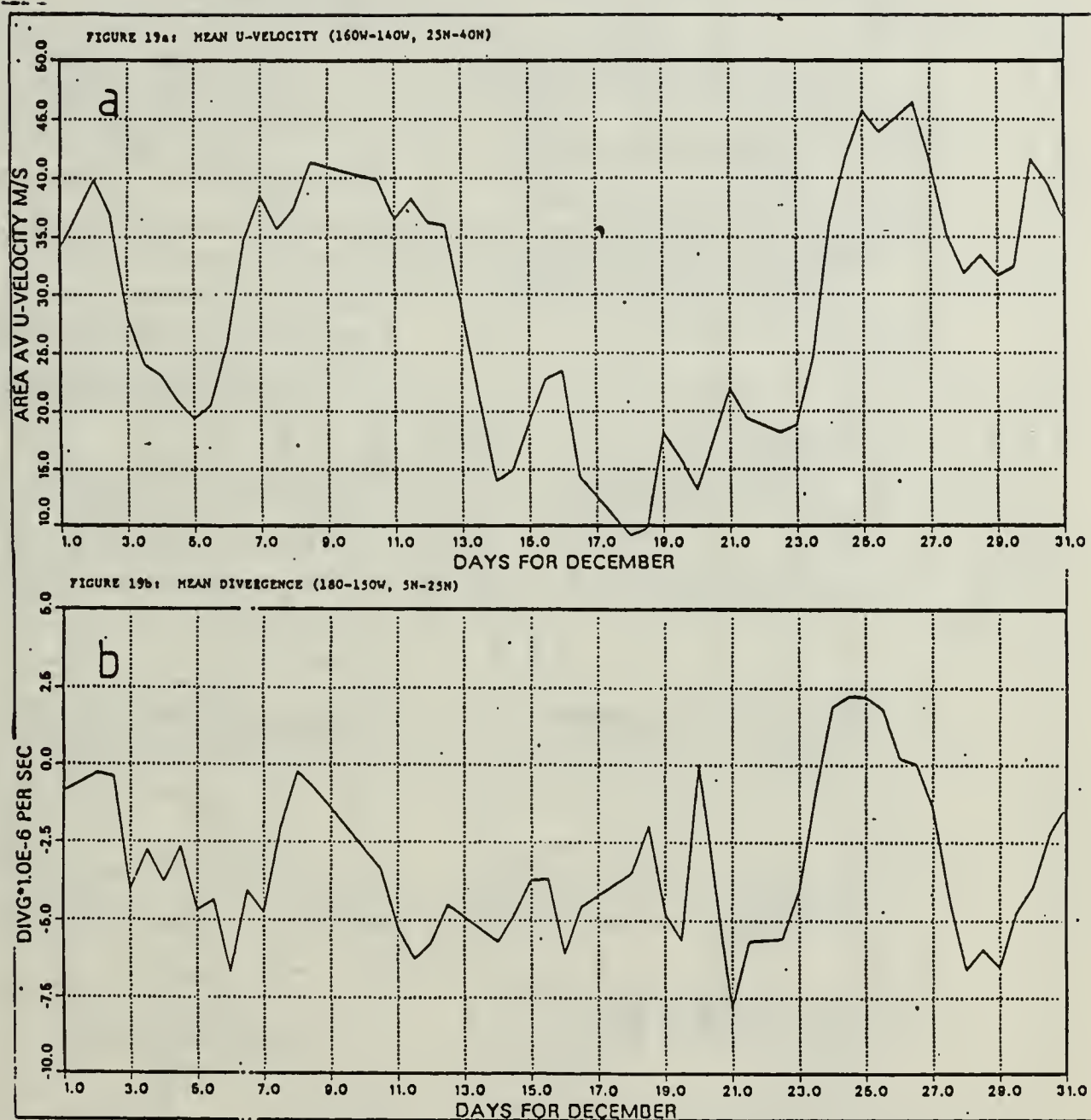


Fig. 19a As in Fig. 11a except for Northern Central Pacific region (NP), (160-140W, 25N-40N)

Fig. 19b As in Fig. 11b except for Tropical Central Pacific region (180-150W, 5N-25N) (CP)

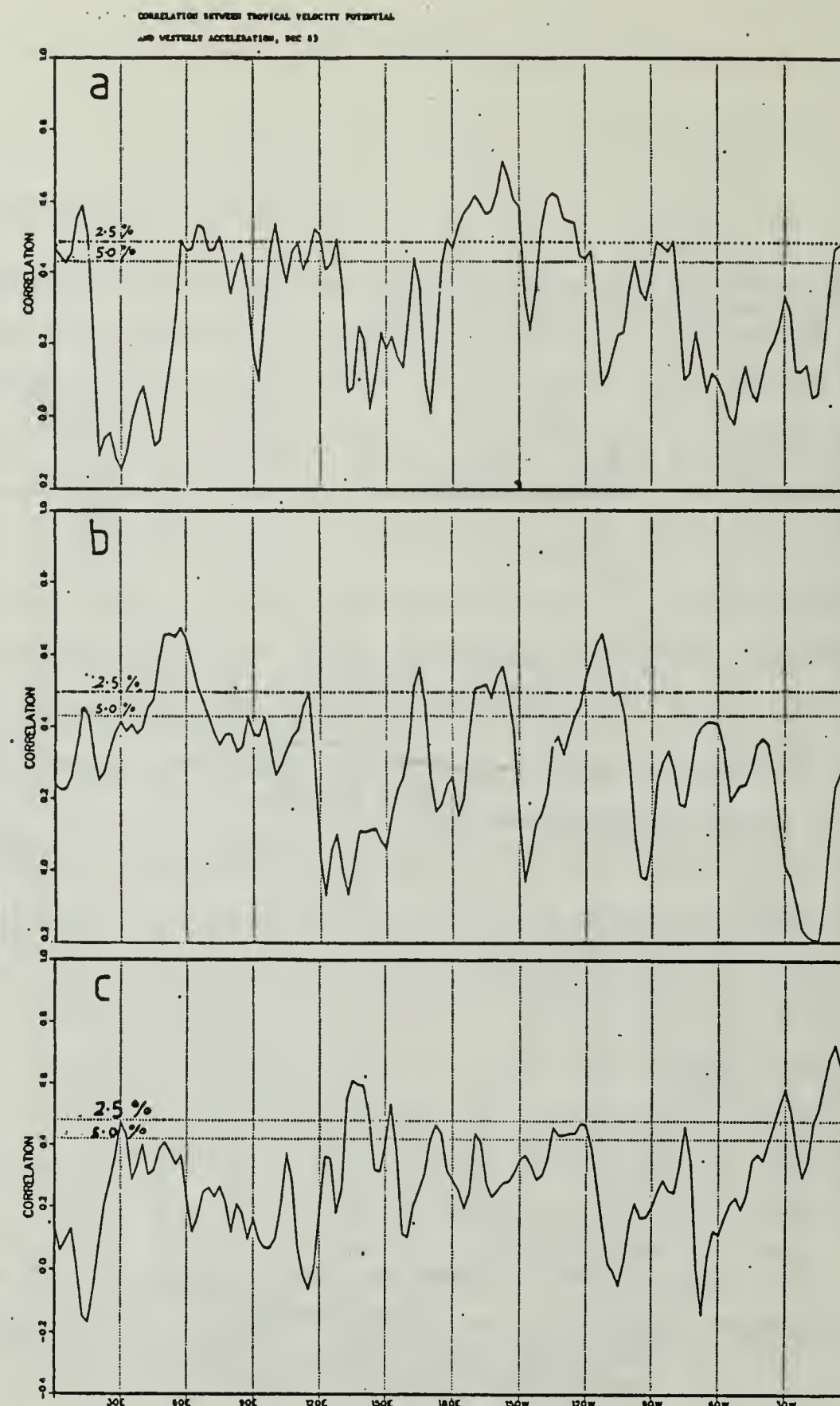


Fig. 20      Correlation between tropical velocity potential  
and westerly acceleration in the midlatitudes  
(a) December 1984 (b) January 1984 and  
(c) February 1984.

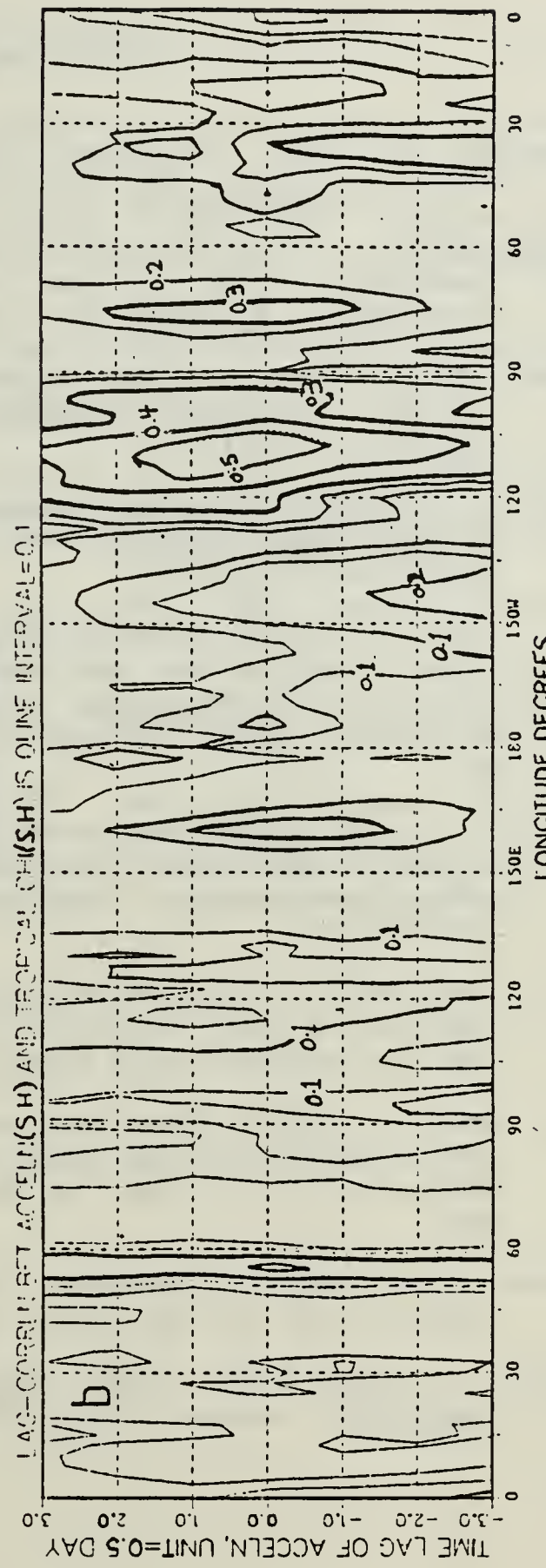
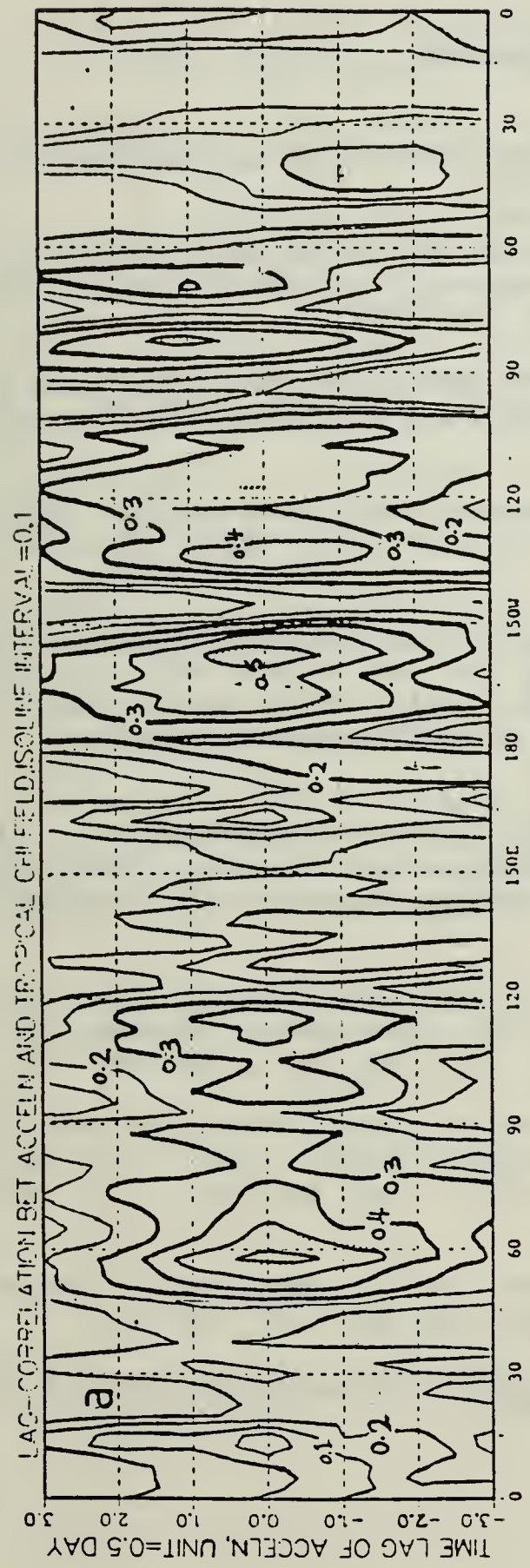


Fig. 21 Time-lag correlation between tropical velocity potential and zonal acceleration in the midlatitudes for (a) northern hemisphere (b) southern hemisphere (1983/84).

## LIST OF REFERENCES

- Bjerknes, J., 1969: Atmospheric teleconnections from the equatorial Pacific, Mon. Wea. Rev., 97, 163-172.
- Blackmon, M. L., J. M. Wallace, N. C. Lau and S. M. Mullen, 1977: On observation study of the Northern Hemisphere winter time circulation. J. Atmos. Sci., 34, 1040-1053.
- Bosart, L. F., 1973: A synoptic investigation of anomalous warmth in the mid and upper troposphere during February 1964. J. Appl. Meteor., 12, 3-11.
- Boyle, J. S., 1983: Synoptic study of the initiation of surges. Report of Winter MONEX Workshop, Monterey, June 1982. Naval Postgraduate School Tech 63-83-002.
- \_\_\_\_\_ and C.-P. Chang, 1984: Monthly and seasonal climatology over the global tropics and subtropics for the decade 1973 to 1983. Volume I: 200 mb winds. Tech. Rep., NPS-63-84-006, Dept. of Meteorology, Naval Postgraduate School, Monterey, CA 93943, 172 pp.
- Chang, C.-P., J. E. Erickson and K. M. Lau, 1979: Northeasterly cold surges and near-equatorial disturbances over the winter MONEX area during December 1974. Part I: Synoptic aspects. Mon. Wea. Rev., 107, 812-829.
- \_\_\_\_\_ and K. M. Lau, 1980: Northeasterly cold surges and near-equatorial disturbances over the Winter MONEX area during December 1974. Part II: Planetary scale aspects. Mon. Wea. Rev., 108, 298-312.
- \_\_\_\_\_ and \_\_\_\_\_, 1982: Short-term planetary-scale interactions over the tropics and midlatitude during northern winter. Part I: Contrasts between active and inactive periods. Mon. Wea. Rev., 110, 933-946.
- Hawkins, H. F. and S. L. Rosenthal, 1965: On the computation of streamfunction from the wind field. Mon. Wea. Rev., 93, 245-252.
- Hoskins, B. and R. Pearce, 1983: Large-Scale Dynamical Processes in the Atmosphere. Academic Press, 397 pp.

- Julian, P. R., 1984: Objective analysis in the tropics: A proposed scheme. Mon. Wea. Rev., 112, 1752-1767.
- Krishnamurti, T. N., 1961: The subtropical jet stream of winter. J. Meteorol., 18, 172-191.
- \_\_\_\_\_, M. Kanamitsu, W. J. Koss, and J. D. Lee, 1973: Tropical east-west circulations during the northern winter. J. Atmos. Sci., 30, 780-787.
- Lau, K. M., C.-P. Chang, P. H. Chan, 1983: Short-term planetary-scale interactions over the tropics and midlatitudes. Part II: Winter-MONEX period. Mon. Wea. Rev., 111, 1372-1388.
- Lim, H. and C.-P. Chang, 1983: Dynamics of teleconnections and Walker circulations forced by equatorial heating. J. Atmos. Sci., 40, 1897-1915.
- Lorenz, E. N., 1967: The nature and theory of the general circulation of the atmosphere. WMO, Geneva, Switzerland.
- Palmen, E. and C. W. Newton, 1969: Atmospheric Circulation Systems. Academic Press, 603 pp.
- Panofsky, H. A. and G. W. Brier, 1968: Some applications of statistics to meteorology. Pennsylvania State University, 224 pp.
- Ramage, C. S., 1971: Monsoon Meteorology. Academic Press, 296 pp.

INITIAL DISTRIBUTION LIST

	No. of copies
1. Defense Technical Information Center Cameron Station Alexandria, VA 22304-6145	2
2. Library, Code 0142 Naval Postgraduate School Monterey, CA 93943-5100	2
3. Professor R. J. Renard, Code 63Rd Naval Postgraduate School Monterey, CA 93943-5100	1
4. Professor C.-P. Chang, Code 63Cp Naval Postgraduate School Monterey, CA 93943-5100	2
5. Professor J. S. Boyle, Code 63Xj Naval Postgraduate School Monterey, CA 93943-5100	2
6. Mr. Keng-Gaik Lum No. 39, Road 14/1 Petaling Jaya, Selangor, Malaysia	4









214365

Thesis

K354

c.1

Keng-Gaik

The influence of  
large-scale 200 mb  
tropical divergence  
events on the midla-  
titude zonal flow over  
the Asia-Pacific re-  
gion during the 1983-  
84 winter.

214365

Thesis

K354

c.1

Keng-Gaik

The influence of  
large-scale 200 mb  
tropical divergence  
events on the midla-  
titude zonal flow over  
the Asia-Pacific re-  
gion during the 1983-  
84 winter.



thesK354

The influence of Large-scale 200 mb trop



3 2768 000 65057 6

DUDLEY KNOX LIBRARY